



**QUEEN'S  
UNIVERSITY  
BELFAST**

## Positron annihilation on large molecules

Iwata, K., Gribakin, G. F., Greaves, R. G., Kurz, C., & Surko, C. M. (2000). Positron annihilation on large molecules. DOI: 10.1103/PhysRevA.61.022719

**Published in:**  
Physical Review A

**Document Version:**  
Peer reviewed version

**Queen's University Belfast - Research Portal:**  
[Link to publication record in Queen's University Belfast Research Portal](#)

### **General rights**

Copyright for the publications made accessible via the Queen's University Belfast Research Portal is retained by the author(s) and / or other copyright owners and it is a condition of accessing these publications that users recognise and abide by the legal requirements associated with these rights.

### **Take down policy**

The Research Portal is Queen's institutional repository that provides access to Queen's research output. Every effort has been made to ensure that content in the Research Portal does not infringe any person's rights, or applicable UK laws. If you discover content in the Research Portal that you believe breaches copyright or violates any law, please contact [openaccess@qub.ac.uk](mailto:openaccess@qub.ac.uk).

## Positron annihilation on large molecules

Koji Iwata,<sup>1\*</sup> G. F. Gribakin,<sup>2</sup> R. G. Greaves,<sup>1†</sup> C. Kurz,<sup>1‡</sup> and C. M. Surko<sup>1§</sup>

<sup>1</sup>*Physics Department, University of California, San Diego, La Jolla, California 92093-0319*

<sup>2</sup>*School of Physics, University of New South Wales, Sydney 2052, Australia*

### Abstract

Positron annihilation on molecules is known to depend sensitively on molecular structure. For example, in the case of hydrocarbon molecules, modest changes in molecular size produce orders of magnitude changes in the observed annihilation rates. Although this process has been studied for more than three decades, many open questions remain. Experimental studies are described which are designed to test specific features of the annihilation process. Two possible mechanisms of the annihilation are considered theoretically: direct annihilation of the positron with one of the molecular electrons, including possible enhancement of this process when low-lying virtual or bound positron-molecule states are present, and resonant annihilation through positron capture into vibrationally excited states of the positron-molecule complex. The dependence of annihilation rates,  $\lambda$ , on positron temperature,  $T_p$ , is studied for the first time for molecules, and at low values of  $T_p$  the dependence follows a power law,  $\lambda \propto T^{-\xi}$ , with  $\xi \approx 0.5$ . These data are used to test the predictions of direct numerical calculations and theories of the virtual-level enhancement. Partially fluorinated hydrocarbons are studied in order to understand the rapid changes in annihilation rate produced in hydrocarbons as a result of fluorine substitution. These data are compared with the behavior expected due to direct annihilation when there is virtual or bound level enhancement. Measurements of positron annihilation on deuterated hydrocarbons are described which test the dependence of the annihilation on the nature of the molecular vibrations. The relationship of the presently available experimental data for annihilation in molecules to current theories of the annihilation process is discussed.

PACS numbers: 34.50.-s, 78.70.Bj, 71.60.+z, 36.10.-k

## I. INTRODUCTION

The annihilation of low-energy positrons on atoms and molecules is a fundamental phenomenon in the field of atomic and molecular physics [1,2]. Experimental studies of this subject have been conducted for more than four decades [3,4]. The introduction of a modified Penning-Malmberg trap a decade ago to accumulate large numbers of room-temperature positrons has expanded experimental capabilities for these studies [5,6]. The quality of the data was further improved by subsequent increases in the number of positrons available for experimentation [2,7]. The variety of substances studied has also expanded due to improvements in the low-pressure operation of the positron accumulator [1,2]. Stored positrons can now be manipulated for other kinds of experiments, including heating the positrons for temperature dependence studies [8,9], and the creation of positron beams with very narrow energy spreads for a new generation of scattering experiments [10]. While these advances and complementary theoretical work have illuminated many facets of the interaction of positrons with atoms and molecules leading to annihilation, a detailed understanding of the phenomenon has yet to be achieved.

Historically, the annihilation rates of positrons with atoms or molecules have been expressed in terms of the dimensionless parameter

$$Z_{\text{eff}} \equiv \frac{\lambda}{\pi r_0^2 cn}, \quad (1)$$

where  $\lambda$  is the observed annihilation rate,  $r_0$  is the classical radius of an electron,  $c$  is the speed of light, and  $n$  is the number density of atoms or molecules [1]. Measured values of  $Z_{\text{eff}}$  for a variety of substances are summarized in Ref. [1]. The parameter  $Z_{\text{eff}}$  is a modification of the Dirac annihilation rate for a positron in an uncorrelated electron gas. For small atoms and molecules,  $Z_{\text{eff}}$  is typically regarded as the effective number of electrons contributing to the annihilation process. For these species, values of  $Z_{\text{eff}}$  are similar to the number of electrons in the atom or molecule,  $Z$ . However this approximation is crude; for example, even for atomic hydrogen, which has only one electron,  $Z_{\text{eff}}$  is 8.0 at low energies [11]. There is extensive evidence that annihilation occurs only on outer-shell electrons [2]. Thus, in the case of large atoms, one should consider that it is not all the electrons but only the valence electrons (e.g., 8 for noble gases heavier than helium) that participate in the annihilation process, yet  $Z_{\text{eff}} = 400$  for Xe. Annihilation rates as much as two orders of magnitude larger than  $Z$  were observed for molecules such as butane by Paul and Saint-Pierre in 1963 [3]. Surko *et al.*, taking advantage of the low-pressure capabilities of the positron trap [5], were able to extend these studies to larger organic molecules, including alkanes as large as hexadecane ( $\text{C}_{16}\text{H}_{34}$ ) and a variety of aromatic molecules, and annihilation rates,  $Z_{\text{eff}}$ , up to five orders of magnitude larger than  $Z$  were observed. Thus, the data clearly indicate that a model of the annihilation process based upon Eq. (1) and uncorrelated dynamics of the positron and bound electrons is inadequate.

While a detailed explanation of the experimental data is still lacking, we believe it is useful to relate the experimental results to two possible mechanisms of the annihilation process. We consider here annihilation in the case where there is a thermal distribution of low energy positrons interacting with atoms or molecules. The simplest mechanism is *direct annihilation* of the incident positron with one of the atomic or molecular electrons. The

contribution of this mechanism to the annihilation rate is proportional to the number of valence electrons available for annihilation. It will be enhanced by the attractive positron-electron interaction which tends to increase the overlap of the positron and electron densities on the atom or molecule. For example, this is the case when a low-lying virtual level at energy  $\varepsilon_0 > 0$  or a shallow bound  $s$  state ( $\varepsilon_0 < 0$ ) exists for the positron [12]. It is known that, in this case,  $Z_{\text{eff}}^{(\text{dir})} \propto 1/(|\varepsilon_0| + \varepsilon)$  for small positron kinetic energies  $\varepsilon \lesssim |\varepsilon_0|$  [13–15]. It has been predicted that this effect is responsible for the large  $Z_{\text{eff}}$  values observed in the heavier noble gases ( $Z_{\text{eff}} = 33.8, 90.1$  and  $401$  for Ar, Kr and Xe, respectively [1,16]).

In the case of annihilation on molecules, which have vibrational and rotational degrees of freedom, a second potentially important mechanism is *resonant annihilation*. In this process, the positron annihilates with a valence electron after being captured into a Feshbach-type resonance in which the positron is bound to a vibrationally excited molecule. In analogy with a mechanism frequently used to explain electron attachment to molecules, this mechanism was advanced [5] to explain the high annihilation rates observed in alkane molecules and the strong dependence of annihilation rates on molecular size. This model assumes that the positron can form bound states with the neutral molecules (i.e., that the positron affinity of the molecule is positive,  $\epsilon_A > 0$ ). Capture is then possible if the positron energy is in resonance with one of the vibrationally excited states of the positron-molecule complex. Such resonances have been observed in electron scattering from some simple molecules, e.g., NO [17], that have positive electron affinities.

The density of states,  $\rho(E)$ , due to the vibrational excitation spectrum of the complex can be high, even if the available energy,  $E = \epsilon_A + \varepsilon$ , is only a few tenths of an electron Volt (making the plausible assumption that the presence of the positron does not alter significantly the molecular vibrational spectrum). For a thermal (i.e., Maxwellian) distribution of positron energies, the observed resonant contribution  $Z_{\text{eff}}^{(\text{res})}$  in large molecules is an average over many resonances located at specific positron energies. Accordingly, the magnitude of  $Z_{\text{eff}}^{(\text{res})}$  is proportional to  $\rho(E)$ . This density of states increases rapidly with the size of the molecule,  $\rho(E) \propto (N_v)^{n_v}$ , where  $N_v$  is the number of vibrational modes and  $n_v \sim \epsilon_A/\omega$  is the effective number of vibrational quanta excited in positron capture with  $\omega$ , a typical molecular vibrational frequency. Thus, the resonant annihilation mechanism provides a possible explanation for the rapid increase in  $Z_{\text{eff}}$  that is observed when the size of the molecule is increased. For thermal positrons, we have estimated that values of  $Z_{\text{eff}}^{(\text{res})}$  as large as  $10^7$ – $10^8$  might be expected as a result of this process. These values are comparable with the largest values of  $Z_{\text{eff}}$  observed so far:  $4.33 \times 10^6$  for anthracene [18], and  $7.56 \times 10^6$  for sebacic acid dimethyl ester [19].

One necessary condition for resonant annihilation is the existence of a positron-molecule bound state. Indirect evidence for the existence of such states comes from the experimental results and their interpretation by Surko *et al.* [5]. Many-body theory calculations by Dzuba *et al.* [20] predict that positrons can be bound to metal atoms such as Mg, Zn, Cd, and Hg. Variational calculations by Ryzhikh and Mitroy proved rigorously that positrons form bound states with Li atoms, and showed that bound states also exist for Na, Be, Mg, Zn and Cu [21]. It is likely that molecules have essentially much larger long-range “potential wells” for the positron, and therefore many molecules are likely to be capable of binding positrons.

The objective of the present study was to try to investigate specific features of the annihilation process by studying the dependence of annihilation rates on such parameters as

positron temperature, the electronic structure of the molecules, and the frequency spectrum of molecular vibrational modes. As discussed below, we have not been entirely successful in this objective. Nonetheless, the studies described here can provide important benchmarks with which to test refined models of the annihilation process.

This paper is organized in the following way. In Sec. II, previous experimental results are reviewed. Theoretical considerations regarding the annihilation process are described briefly in Sec. III. The positron trap and the experimental procedure for measuring annihilation rates are described in Sec. IV. The results of a new series of experiments and the relationship of these studies and other available data to current theoretical work are discussed in Sec. V. We also test a recently proposed phenomenological model of the annihilation process in Sec. V D. Finally, our current understanding of the physics involved in the positron annihilation processes is summarized in Sec. VI, together with a discussion of open questions in this area.

## II. PREVIOUS EXPERIMENTS

The existence of very high annihilation rates on large molecules was discovered in the early sixties in the seminal work of Paul and Saint Pierre [3] and complementary experiments were later carried out by Heyland *et al.* [4]. Later, Surko *et al.* used a positron accumulator to extend these studies to much larger molecules [5]. Murphy and Surko discovered very strong dependences of the rates of positron annihilation on the chemical composition of the molecules. For example, they found that perfluorinated molecules have much smaller annihilation rates than those of the analogous hydrocarbons [18]. They also discovered an empirical linear scaling of  $\ln(Z_{\text{eff}})$  with  $(E_i - E_{\text{Ps}})^{-1}$ , where  $E_i$  is the atomic or molecular ionization potential, and  $E_{\text{Ps}} = 6.8$  eV is the binding energy of a positronium atom (Ps).

This scaling was found to be valid (to better than an order of magnitude in  $Z_{\text{eff}}$ ) for all noble-gas atoms and non-polar molecules studied thus far (i.e., species in which  $E_i > E_{\text{Ps}}$ ), that do not contain double or triple bonds. While this scaling has not been understood theoretically, it has been conjectured that it provides evidence for a model in which a highly correlated electron-positron pair moves in the field of the resulting positive ion, and that this dominates the physics of the annihilation process [18].

Recent theoretical work on positron annihilation with noble gas atoms [15] and ethylene [22] confirms that virtual Ps formation gives a large contribution to the positron-atom and positron-molecule attraction, and is crucial for determining the low-lying virtual levels for the positron that give rise to large  $Z_{\text{eff}}$  values. However, if the ionization energy of the system is greater than  $E_{\text{Ps}}$  by one or a few eV, the Ps-formation process is strongly virtual (i.e., far off the energy shell), and consequently the lifetime of this temporary “ion+Ps” state,  $\tau \sim \hbar/(E_i - E_{\text{Ps}})$  is not large enough to produce any direct effect on the positron-atom or positron-molecule complex.

In a separate set of experiments, the spectra of 511-keV  $\gamma$  rays from positrons annihilating on various atoms and molecules were studied in a positron trap [2]. The observed spectra are Doppler broadened due to the momentum distribution of annihilating electron-positron pairs which, for the case of room-temperature positrons, is dominated by the momentum distribution of the bound electrons [23]. Thus the Doppler broadening measurements provide information about the quantum states of the annihilating electrons. The results obtained in

Ref. [2] are consistent with a model in which the positrons annihilate with equal probability on any valence electron (i.e., a model in which the positron density is distributed evenly around the molecule). These measurements indicate that the large annihilation rates that are observed depend on global properties of the molecule as opposed to (localized) positron affinity to a particular atomic site.

### III. THEORETICAL CONSIDERATIONS

In a paper now in preparation, Gribakin discusses two basic mechanisms of positron annihilation, direct and resonance annihilation, that are potentially relevant to the interaction of low-energy positrons with molecules [24]. Here, we briefly summarize the key results of this analysis.

The physical processes responsible for the observed large values of  $Z_{\text{eff}}$  can be understood qualitatively in the following way. The interaction rate,  $\lambda_i$ , of a positron with an atom or a molecule can be expressed as  $\lambda_i = n\sigma v$ , where  $\sigma$  is the interaction cross section and  $v$  is the velocity of the positron relative to the atom or molecule. If the positron-atom or positron-molecule interaction time (or the “dwell time”) is denoted by  $\tau$ , the probability of the positron annihilating during an interaction can be written heuristically as  $(1 - e^{-\tau/\tau_a})$ , where  $1/\tau_a \equiv \Gamma_a$  is the annihilation rate for the positron localized near the atom or molecule during the interaction. It is obtained from the two-photon spin-averaged annihilation cross section as

$$\Gamma_a = \pi r_0^2 c \rho_{ep}, \quad (2)$$

where  $\rho_{ep}$  is the positron density on the atomic or molecular electrons [25]. If we use  $\rho_{ep} = 1/(8\pi a_0^3)$  for the ground-state Ps atom as an estimate, then  $\tau_a \approx 5 \times 10^{-10}$  s is the familiar spin-averaged Ps lifetime. Thus, the annihilation rate  $\lambda$  in positron-atom or positron-molecule interactions is given by

$$\lambda = n\sigma v(1 - e^{-\tau/\tau_a}). \quad (3)$$

Comparing this expression with the definition of  $Z_{\text{eff}}$ , Eq. (1), we have

$$Z_{\text{eff}} = \frac{\sigma v}{\pi r_0^2 c} (1 - e^{-\tau/\tau_a}). \quad (4)$$

Therefore, enhanced values of  $Z_{\text{eff}}$  can be achieved by either having large interaction cross section  $\sigma$ , or by making the interaction time  $\tau$  large.

In this section, we discuss cases in which the interaction of positrons with atoms and molecules can result in relatively large value of  $\sigma$  or  $\tau$ . We first discuss direct annihilation in atoms and molecules. We then discuss resonant annihilation in molecules that possess vibrational and rotational degrees of freedom. Finally, we discuss the circumstances by which molecules with several atoms are likely to have virtual or weakly bound levels, which in turn, can have an important effect on the annihilation process.

We have omitted from discussion two other possible mechanisms which lead to formation of quasibound (or bound) positron-atom or positron-molecule states (i.e., states that would produce large values of  $\tau$ ). Formation of a bound state is energetically prohibited in a

two-body collision, and so another particle is necessary. We discuss below the case where vibrational excitations (i.e., phonons) play the role of the third particle. Other possible mechanisms involve another atom or molecule in the collision (i.e., three-body collision) or a photon. We do not discuss the possibility of three-body collisions involving the positron and two atoms or molecules because our experiments are performed at low pressures of the test gas, and the annihilation rates are observed to depend linearly on test-gas pressure [1]. This indicates that the annihilation process is due to a two-body interaction of a positron and an atom or a molecule.

The positron-atom or positron-molecule quasibound state formed by positron capture could be stabilized by the emission of a photon. However, the radiative lifetime for infrared emission is much larger than typical atomic radiative lifetimes, and so it is also much larger than the positron annihilation lifetime in the atom or molecule. The annihilation event has a much greater probability than radiative stabilization. The positron could also be captured into a true bound state in a binary collision with the atom or molecule by the emission of a photon (i.e., “radiative recombination”). In this case,  $\sigma$  in Eq. (4) would be the radiative recombination cross section, and  $\tau$  in Eq. (4) would be infinite. However, it can be shown that the probability of this process has the same order in inverse powers of  $c$  as direct positron annihilation. Numerically, this gives a contribution to  $Z_{\text{eff}}$  which is less than 1. Since this effect does not increase rapidly with the size of the molecule, it also appears to be negligible.

One feature of the available data runs counter to the idea that different annihilation mechanisms are operative for different classes of atomic and molecular species. As we have reported previously and discuss in Sec. VD 1, there is an empirical scaling of the form  $\ln(Z_{\text{eff}}) = A(E_i - E_{\text{Ps}})^{-1}$ , which fits all of the data for atoms and single-bonded molecules reasonably well, with only one fit parameter,  $A$ . This scaling could be interpreted as evidence that one mechanism describes annihilation in both atoms and molecules. In this picture, the major differences in annihilation rates are due only to differences in the electronic structure of the atoms and molecules (i.e., in contrast to the resonant vibrational mode model discussed above). Thus, one mechanism would be responsible for both small and large values of  $Z_{\text{eff}}$ . However, we are not aware of any existing theoretical picture that could explain the large observed values of annihilation rates on the basis of electronic structure alone. Consequently, we present here a theoretical framework in which different annihilation mechanisms are dominant for different classes of atomic and molecular species, but we encourage further investigation of this issue.

### A. Direct annihilation

Suppose first that the positron-atom or positron-molecule interaction is a simple elastic collision and the annihilation takes place directly between the incident positron and one of the bound electrons. The dwell time  $\tau \sim R_a/v$ , where  $R_a$  is the atomic or molecular radius, is small compared to the annihilation time  $\tau_a$ . Hence, the annihilation probability is just  $\tau/\tau_a \ll 1$ , and the rate of direct annihilation is estimated as

$$Z_{\text{eff}}^{(\text{dir})} \sim \sigma R_a \rho_{ep} , \quad (5)$$

where we used Eq. (2) to estimate  $\tau_a$ . If we consider a typical low-energy positron-atom or positron-molecule cross section in the range  $\sigma = 10^{-15}\text{--}10^{-14}$  cm<sup>2</sup>,  $R_a = 5a_0$  and the Ps value of  $\rho_{ep}$ , then  $Z_{\text{eff}}^{(\text{dir})} \sim 10\text{--}100$  is obtained.

The long-range positron-atom or positron-molecule interaction is attractive due to dipole polarization of the electron cloud by the positron. At low incident energies this interaction may increase the collision cross section  $\sigma$  above the value determined by the geometric size of the atom or molecule, if a virtual ( $\kappa < 0$ ) or a shallow bound ( $\kappa > 0$ )  $s$  state exists for the positron-atom or positron-molecule system at  $\varepsilon_0 = \pm\hbar^2\kappa^2/2m$ . In this situation the scattering length  $a = \kappa^{-1}$  and the cross section at zero energy  $\sigma = 4\pi a^2 = 4\pi\kappa^{-2}$  can be much greater than the size of the atom or molecule [13,26]. This effect can explain the rapid increase and large values of  $Z_{\text{eff}}$  in Ar, Kr and Xe [14,15]. The enhancement due to this mechanism is limited by the size of the positron wavelength. For room-temperature positrons the wave number is  $k \sim 0.045a_0^{-1}$ , and the maximal possible cross section  $\sigma \simeq 4\pi k^{-2}$  corresponds to  $Z_{\text{eff}}^{(\text{dir})} \sim 10^3$ . This value of  $Z_{\text{eff}}$  is still much smaller than the values observed for large molecules. We conclude that the positron dwell time near the molecule,  $\tau$ , must be much larger than that of the simple direct annihilation process.

Equation (5) is too simple to describe direct annihilation quantitatively. However, it is possible to derive a more accurate formula that relates  $Z_{\text{eff}}^{(\text{dir})}$  to the scattering properties of the system at low positron energies [24]:

$$Z_{\text{eff}}^{(\text{dir})} \simeq F \left( R_a^2 + \frac{\sigma}{4\pi} + 2R_a \text{Re}f_0 \right), \quad (6)$$

where  $\sigma$  is the elastic cross section,  $f_0$  is the  $s$ -wave scattering amplitude,  $R_a$  is the average positron-atom or positron-molecule separation at which the annihilation occurs, and  $F$  is a factor that takes into account the overlap of the positron and electron densities. Note that unlike Eq. (5), the above expression does not vanish even when the scattering cross section is very small. Indeed, the positron wave function is always a sum of the incident and scattered waves, and even if the scattering amplitude is very small, the incident wave contributes to the annihilation rate. Formula (6) contains contributions of both, as well as the interference term. When the scattering cross section is anomalously large,  $|a| \gg R_a$ , Eq. (6) coincides with Eq. (5). Comparison of theoretical cross sections and  $Z_{\text{eff}}$  for noble gases [27] and C<sub>2</sub>H<sub>4</sub> [22] shows that Eq. (6) works well at energies of up to 0.5 eV, if  $R_a$  and  $F$  are used as fitting parameters ( $R_a \sim 4$  and  $F \sim 1$  a.u. are the typical values). When low-energy scattering is dominated by the presence of a virtual level or a weakly bound  $s$  state, both  $\sigma$  and  $Z_{\text{eff}}$  become large. They also show a similar rapid dependence on the positron momentum. For a short-range potential, this dependence is determined by the standard formulae [28]

$$f_0 = -\frac{1}{\kappa + ik}, \quad \sigma = \frac{4\pi}{\kappa^2 + k^2}. \quad (7)$$

Since the target has a non-zero dipole polarizability  $\alpha$ , these formulae must be modified to account for the long-range  $-\alpha e^2/2r^4$  positron-target interaction. This can be done by using the modified effective-range expression for the  $s$ -wave phase shift  $\delta_0$

$$\tan \delta_0 = -ak \left[ 1 - \frac{\pi\alpha k}{3a} - \frac{4\alpha k^2}{3} \ln \left( C \frac{\sqrt{\alpha k}}{4} \right) \right]^{-1}, \quad (8)$$



together with the usual relations  $\sigma = 4\pi \sin^2 \delta_0/k^2$  and  $\text{Re}f_0 = \sin 2\delta_0/2k$  (atomic units  $\hbar = m = e = 1$  are used hereafter) [29]. If  $\alpha$  is known, Eq. (8) contains basically one free parameter, the scattering length  $a$ , since the dependence of  $\delta_0$  on the positive constant  $C$  is rather weak. For  $\alpha = 0$  Eq. (7) with  $\kappa = a^{-1}$  are recovered. The polarization potential changes qualitatively the behavior of  $\sigma$  and  $Z_{\text{eff}}$  at small momenta. They now contain terms linear in positron momentum  $k$ , and  $\sigma = 4\pi(a + \pi\alpha k/3)^2$  follows from Eq. (8) in the case where  $k \rightarrow 0$  and  $|a| \gg \pi\alpha k/3$ .

To describe annihilation of thermal positrons, one must fold  $Z_{\text{eff}}(k)$  with the Maxwellian distribution at temperature  $T$ , and the result is

$$Z_{\text{eff}}(T) = \int_0^\infty Z_{\text{eff}}(k) \exp\left(-\frac{k^2}{2k_B T}\right) \frac{4\pi k^2 dk}{(2\pi k_B T)^{3/2}}. \quad (9)$$

At room temperature  $T = 293$  K the typical positron energies are  $k^2/2 \sim k_B T = 9.3 \times 10^{-4}$  a.u., which corresponds to thermal positron momenta  $k \approx 0.045$ .

## B. Resonant annihilation

The interaction time  $\tau$  can be made much greater if the low-energy positron is captured by the molecule in a process involving the excitation of a narrow resonance in the positron-molecule system. Enhancement of annihilation due to the excitation of a single resonance was considered theoretically in [26] and [30]. The possibility of forming such resonances by excitation of the vibrational degrees of freedom of molecules was discussed by Surko *et al.* [5]. Suppose that the positron affinity,  $\epsilon_A$ , of the molecule is positive (e.g.,  $\epsilon_A$  is a fraction of an electron Volt). Vibrationally excited states of the positron-molecule complex would then manifest as resonances in the positron continuum, and provide a path for resonant annihilation. In this process the positron is first trapped temporarily by the molecule. In this case, there are two possibilities. The positron can annihilate with one of the molecular electrons or it can undergo detachment and return to the continuum. As a result, the resonant annihilation rate  $\lambda^{(\text{res})}$  is proportional to the probability of positron capture multiplied by the probability of its annihilation in the quasibound state.

A positron-molecule resonance is characterized by its total line width  $\Gamma = \Gamma_a + \Gamma_c$ , where  $\Gamma_a$  and  $\Gamma_c$  are the rates (or partial widths) for annihilation and capture, respectively. These quantities are directly related to the lifetime of the resonant state against annihilation,  $\tau_a = 1/\Gamma_a$ , and positron detachment,  $\tau_c = 1/\Gamma_c$ , and  $\tau$  in Eq. (4) is  $1/\Gamma$ . The probability of annihilation in the resonant state is determined by the competition of these two processes:  $P_a = \Gamma_a/(\Gamma_a + \Gamma_c)$ . The resonant annihilation rate is given by

$$\lambda^{(\text{res})} = n\sigma_c v P_a, \quad (10)$$

where  $\sigma_c$  is the capture cross section. If the molecule absorbed all incoming positrons,  $\sigma_c$  would be equal to the so-called Langevin cross section  $\sigma_L = \pi\lambda^2 = \pi k^{-2}$ . This cross section corresponds to the *s*-wave capture, which dominates at low positron energies. The true capture cross section is smaller than  $\sigma_L$ , because the capture takes place only when the positron energy matches the energy of the resonance. For positrons with a finite energy spread (e.g., thermal), the capture cross section is then  $\sigma_c \sim (\Gamma_c/D)\sigma_L$ , where  $D$  is the

mean energy spacing between the resonances. More accurately,  $\sigma_c = (2\pi\Gamma_c/D)\sigma_L$  [28], and Eq. (10) yields [24]

$$\lambda^{(\text{res})} = n \frac{\pi}{k^2} \frac{2\pi\Gamma_c}{D} k \frac{\Gamma_a}{\Gamma_a + \Gamma_c}, \quad (11)$$

( $v = k$  in atomic units). Using Eq. (2) and the definition of  $Z_{\text{eff}}$  we obtain

$$Z_{\text{eff}}^{(\text{res})} = \frac{2\pi^2}{k} \frac{\rho_{ep}\Gamma_c}{D(\Gamma_a + \Gamma_c)} \equiv \frac{2\pi^2}{k} \frac{\rho_{ep}\tau_a}{D(\tau_a + \tau_c)}. \quad (12)$$

This expression estimates the average contribution of resonant capture to the positron-molecule annihilation. It becomes especially simple if the capture width is greater than the annihilation width,  $\Gamma_c \gg \Gamma_a \sim 1 \mu\text{eV}$ , or  $\tau_a \gg \tau_c$ :

$$Z_{\text{eff}}^{(\text{res})} = \frac{2\pi^2}{k} \frac{\rho_{ep}}{D}. \quad (13)$$

Therefore, the contribution of resonances to the annihilation rate is proportional to the density of positron-molecule resonances  $\rho(E) = D^{-1}$ , evaluated at the energy released when the positron binds to the molecule,  $E \approx \epsilon_A + k^2/2$ .

Suppose the resonances correspond to vibrationally excited states of the positron-molecule complex, and a single vibrational mode with frequency  $\omega$  is excited. Then we estimate  $D = \omega \sim 0.1 \text{ eV} \sim 4 \times 10^{-3} \text{ a.u.}$ , and for thermal positrons,  $k = 0.045 \text{ a.u.}$ , Eq. (13) gives  $Z_{\text{eff}}^{(\text{res})} \approx 4 \times 10^3$ . In larger molecules several vibrational modes can be excited, and the resonance spectrum density  $D^{-1}$  is much higher. Thus, resonant annihilation can lead to very large values of  $Z_{\text{eff}}$ . However, they cannot be arbitrarily large. The theoretical maximum is achieved in Eq. (12) at  $D \sim \Gamma_c \sim \Gamma_a$ , and it yields  $Z_{\text{eff}}^{(\text{res})} \sim 10^8$  for room temperature positrons. Of course, some of the modes may not be excited in the positron capture due to symmetry constraints, and others may have very small coupling to the positron-molecule channel [small  $\Gamma_c$  in Eq. (12)]. In the latter case the positron-molecule resonant states will have very large lifetimes against positron detachment. However, this does not mean that they contribute much to  $Z_{\text{res}}$ ; if  $\tau_c \rightarrow \infty$  their contribution is very small, since they are effectively decoupled from the positron-molecule continuum, meaning  $\sigma_c \rightarrow 0$ .

Another interesting property of resonant annihilation is an apparent violation of the  $1/v$  law that governs the cross sections of inelastic processes at vanishing projectile energies [28]. This law means that the corresponding rate should be constant at low  $k$ , whereas Eqs. (12) and (13) indicate a  $1/k$  increase of the rate towards zero positron momenta (and a  $E^{-1}$  dependence of the annihilation cross section). This apparent contradiction is resolved if we recall that the capture width  $\Gamma_c$  is also a function of the projectile energy. For  $s$ -wave capture,  $\Gamma_c \propto kR_a$ . Hence Eq. (13) becomes invalid at very small positron momenta, while the complete expression (12) approaches a constant value. The contribution of partial waves with higher orbital momenta  $l$  to the resonant annihilation have the structure of Eq. (12) times a  $2l + 1$  factor. However, the corresponding capture widths behave as  $\Gamma_c \propto (kR_a)^{2l+1}$ . Hence, at low positron energies the  $s$ -wave contribution dominates, and the contribution of  $l \geq 1$  become noticeable only at higher positron energies – first the  $p$  wave, then  $d$  wave, etc.

The  $s$ -wave resonant annihilation's behavior of  $1/k$  means a  $T^{-1/2}$  temperature dependence. This law breaks down for very small  $k$  (or  $T$ ), where  $Z_{\text{eff}}$  becomes constant. Higher

partial waves contributions ( $p, d, \dots$ ) emerge as  $T, T^2$ , etc. at small  $T$ . The latter statement is valid for the direct contribution to  $Z_{\text{eff}}$  as well.

Qualitatively resonant annihilation is similar to electron-molecule attachment. The treatment of Christophorou *et al.* [31,32] for electron-molecule collisions, assumes that the light particle (in their case, the electron) distributes its kinetic energy statistically over the vibrational modes of the molecule. Their treatment provides a way to estimate the capture lifetime in the limit of complete mixing of the vibrational modes. However, a complete quantum-mechanical expression for the positron annihilation rate averaged over the resonances has the form of Eq. (12), and depends on the density of the resonant spectrum  $D^{-1}$ , as well as on the relation between the widths of the competing processes, which for positron annihilation, are  $\Gamma_c$  and  $\Gamma_a$ .

### C. Virtual and weakly bound positron-molecule states

As we have discussed in Sec. III A, the existence of virtual or weakly bound states leads to enhanced direct annihilation rates for both atoms and molecules. Positron-atom or positron-molecule binding is also a necessary condition for resonant annihilation which can result in very high values of  $Z_{\text{eff}}$ . In this section we consider a simple model of a positron interacting with a molecule composed of several atoms. This model illustrates how the chemical composition of the molecule can influence the binding, thereby changing significantly the molecular annihilation rate. We discuss specifically the case of methane and its fluoro-substitutes.

Let us approximate the interaction between a low-energy positron and an atom by the zero-range potential [33]. This potential is characterized by a single parameter  $\kappa_0$ , which determines the behavior of the positron wave function at small distances,

$$\frac{1}{r\psi} \frac{d(r\psi)}{dr} \simeq -\kappa_0. \quad (14)$$

For this potential the  $s$ -wave scattering amplitude is

$$f = -\frac{1}{\kappa_0 + ik}, \quad (15)$$

where  $k$  is the positron momentum, and the scattering length is given as  $a = 1/\kappa_0$ . If  $\kappa_0 > 0$ , there is a bound state at  $E = -\kappa_0^2/2$  (atomic units are used throughout), and  $\kappa_0 < 0$  corresponds to a virtual level.

When we consider low-energy scattering or a weakly bound state for  $n$  scattering centers (atoms), each scattering center can be approximated by a zero-range potential with  $\kappa_i = 1/a_i$ , where  $a_i$  is the scattering length of the  $i$ th atom ( $i = 1, \dots, n$ ). For this system, the eigenvalue problem is reduced to the following algebraic equation for  $\kappa$ ,

$$\det \left| \delta_{ij}(\kappa_i - \kappa) + \frac{\exp(-\kappa R_{ij})}{R_{ij}}(1 - \delta_{ij}) \right| = 0, \quad (16)$$

where  $R_{ij}$  is the distance between atoms  $i$  and  $j$ . Depending on the sign of  $\kappa$ , Eq. (16) can yield either a true bound state,  $E = -\kappa^2/2$  ( $\kappa > 0$ ), or a virtual level,  $E = \kappa^2/2$  ( $\kappa < 0$ ).

The case  $n = 2$  was considered in detail in [34]. This model was also used to investigate positron binding to small xenon clusters [14].

If the atoms form a symmetric configuration, Eq. (16) can be simplified. For example, for  $n = 2, 3$  or 4 identical atoms ( $\kappa_i \equiv \kappa_0$ ) separated by equal distances  $R$  (a diatomic molecule, triangle or tetrahedron configuration), the lowest eigenstate is found from the simple transcendental equation

$$\kappa - (n - 1) \frac{e^{-\kappa R}}{R} = \kappa_0 . \quad (17)$$

We note that even if none of the individual atoms possesses a bound state ( $\kappa_i < 0$  for all  $i$ ), the system of several atoms may well support a bound state. One can easily see this from Eq. (17), which has a positive  $\kappa$  solution for  $(n - 1)/R > -\kappa_0$ .

Let us use the zero-range potential model to consider positron binding to the methane molecule and its fluorinated counterparts ( $\text{CH}_4$  to  $\text{CF}_4$ ). The positron cannot penetrate very deeply into the molecule because of the repulsion from atomic nuclei, and we neglect the effect of the central carbon atom in these compact, rounded-shape molecules. The  $\kappa_0$  parameters of the zero-range potentials for hydrogen and fluorine can be taken from positron-atom calculations. For hydrogen  $\kappa_{\text{H}} = -0.5$  is derived from the positron scattering length  $a = -2.1$  [35]. The value for fluorine can be roughly estimated as  $\kappa_{\text{F}} = -2$  by using the positron scattering length for Ne,  $a = -0.43$  [15,27]. As shown by calculations for heavier halogens [36], their scattering lengths are close to those of the neighboring noble-gas atoms. The interatomic distances  $R_{ij}$  are derived from the geometrical parameters given in [37]. Using these values, Eq. (16) is solved numerically for  $\kappa$ . In the two simplest cases,  $\text{CH}_4$  and  $\text{CF}_4$ , Eq. (17) can be used with  $n = 4$ . For  $\text{CH}_4$  we take  $\kappa_0 = -0.5$ ,  $R = 3.38$  a.u. and obtain  $\kappa = 0.111$ , and for  $\text{CF}_4$  we use  $\kappa_0 = -2$ ,  $R = 4.07$  a.u., and the result is  $\kappa = -0.217$ . Thus, a tetrahedral configuration of four hydrogen atoms provides a bound state for the positron, whereas that of fluorine atoms does not.

The calculated values of  $\kappa$  for all five  $\text{CH}_{4-x}\text{F}_x$  molecules are given in Table I. We see that only the two first members of the series have bound states, whereas for the molecules with 2, 3 and 4 fluorine atoms the binding does not take place, because the fluorine atoms are less attractive for the positron than hydrogen. In all cases the corresponding scattering lengths  $a = 1/\kappa$  are large, which justifies the use of the zero-range potential model. If we use the simple estimate of the direct annihilation rate, Eq. (5) combined with Eq. (7), we conclude that  $Z_{\text{eff}}$  should peak “between”  $\text{CH}_3\text{F}$  and  $\text{CH}_2\text{F}_2$ , in accord with the experimental results (i.e., see Sec. V B). This is an indication that larger alkane molecules are likely to be able to form bound states with positrons, whereas their perfluorinated analogues are probably not capable of positron binding. The implication of this result is that the model predicts that annihilation rates of large alkanes could be determined by resonant annihilation. If so, the annihilation rates for these species are expected to be orders of magnitude greater than those of the perfluorinated alkanes, since only direct annihilation is possible for perfluorinated alkanes because their positron affinities are negative.

## IV. EXPERIMENT

The experiments were performed using a technique similar to previous studies [1,5,18]. However, ongoing refinements in the trapping techniques have substantially enhanced the quality of the data. A schematic diagram of the experiment is shown in Fig. 1. Positrons, emitted at high energies from a 60-mCi  $^{22}\text{Na}$  radioactive source, are moderated to a few eV by a solid neon moderator [38,39]. They are then guided magnetically into a modified three-stage Penning-Malmberg trap. A magnetic field ( $\sim 1$  kG) produced by a solenoid provides positron confinement in the radial direction, and an electrostatic potential well imposed by an electrode structure provides confinement in the axial direction. The positrons experience inelastic collisions with nitrogen buffer gas molecules introduced into the electrode structure and become trapped in the electrostatic potential well. In a time of the order of one second, the trapped positrons cool to room temperature through vibrational and rotational excitation of nitrogen molecules. The trap is designed to accumulate an optimal number of positrons with minimal losses from annihilation on the buffer gas molecules. More detailed accounts of the operation of the positron trap are given elsewhere [40,41].

The positrons end up in the final stage of the trap, which is shown in Fig. 1. A cold surface in the vacuum system is chilled with a water-ethanol mixture to  $-7^\circ\text{C}$  in order to reduce impurities. The base pressure of our system is typically  $5 \times 10^{-10}$  torr, and the positron lifetime with the buffer gas turned off is typically 180 s. The cold surface can be cooled with liquid nitrogen, resulting in positron lifetimes exceeding 1 hour. However, this is not useful for the experiments described here, since most of the gases under study condense on surfaces at liquid nitrogen temperature.

For annihilation-rate measurements, the test substances are introduced into the final stage of the trap as gases at pressures less than  $10^{-6}$  torr. Substances that exist as liquids at room temperature are introduced as low-pressure vapors. Use of low-pressure test gases ensures that the process studied here is dominated by binary encounters of the positrons and atoms or molecules. Annihilation rates are measured by the following procedure. Positrons are accumulated for a fixed time, and then the positron beam is shut off. The positrons are stored in the positron trap for a few seconds in the presence of the test atoms or molecules and then dumped onto a collector plate (Fig. 1). The intensity of the  $\gamma$ -ray pulse from the annihilating positrons is measured. The annihilation lifetime is measured by repeating this procedure for various values of the positron storage time in the presence of the gas. The measurements are performed for various test-gas pressures. The slope of the plot of annihilation time versus pressure is proportional to the (normalized) annihilation rate of the test atoms or molecules. A more detailed account of this technique can be found in Ref. [1].

The dependence of annihilation rate on positron temperature was measured with the technique described in Ref. [9]. This experiment consists of repeated cycles of positron filling, heating the positrons by applying RF noise, and monitoring the subsequent annihilation. After positron filling, the positron beam is switched off, and the trapped positrons cool down to room temperature. The buffer gas is then switched off and pumped out. After a delay time to ensure that the buffer gas density is negligible, the test gas is admitted to the trap. Following an appropriate time delay (to allow the pressure to stabilize), the positrons are heated by applying a pulse of broadband RF noise to one of the confining electrodes. The positrons are heated to temperatures in the range 0.1–0.5 eV for atomic test gases and 0.1–

0.3 eV for molecular test gases (where the maximum temperature is limited by vibrational excitation of the gas molecules). The positrons then cool by collisions with the test gas atoms or molecules after the RF noise is off. Concurrent with the cooling, the positrons annihilate on the test gas while the annihilation is measured using a NaI(Tl) detector to count the  $\gamma$  rays. Before and after each run, the positron temperature is measured as a function of elapsed time since the end of the heating pulse. This is accomplished by reducing the depth of the confining well to zero and analyzing the number of positrons escaping the trap as the function of well depth. A more detailed account of this type of measurement is presented in Ref. [9].

## V. RESULTS

In Sec. V A, we present experimental measurements of positron annihilation rates of deuterated alkanes and the corresponding protonated alkanes. The annihilation rates of alkanes and benzenes with varying degrees of fluorination are presented in Sec. V B. The dependence of annihilation rates of noble gases, hydrocarbons, and fluorinated methanes on positron temperature is described in Sec. V C.

The data presented here differ in certain instances from those reported previously [1]. The values of  $Z_{\text{eff}}$  reported here are larger than the previous measurements by as much as 50%, due to a faulty ion gauge. However, the same gauge is used for all the data sets presented here, so the relative error is expected to be of the order of 10%. Since the models discussed in this paper are compared with the relative values of  $Z_{\text{eff}}$  measured with the same ion gauge, the conclusions reached remain valid in spite of the uncertainties in the absolute values of  $Z_{\text{eff}}$ . Where two values of  $Z_{\text{eff}}$  are reported, those in Ref. [1] are more accurate.

### A. Comparison of annihilation rates for deuterated and protonated hydrocarbons

The annihilation rates of deuterated and protonated alkanes were measured systematically, and the results are listed in Table II. The ratio of  $Z_{\text{eff}}$  for deuterated alkanes to those for protonated alkanes is listed in the last column of the table and is plotted in Fig. 2. As can be seen from the figure, the annihilation rates for the deuterated and protonated alkanes are very similar if not identical. A factor of 2–3 change in annihilation rate was observed previously for deuterated benzenes [1]. However, in contrast to data for the benzenes, the systematic study of alkanes presented here does not provide support for a mechanism in which the positron forms long-lived vibrationally excited resonant states with molecules.

This result would be natural if the annihilation process involved only electron-positron degrees of freedom and proceeded by direct annihilation as described in Sec. III A. This mechanism is likely to dominate for smaller molecules with moderate  $Z_{\text{eff}}$  and relatively high vibrational frequencies and for those with negative positron affinities (like perfluorocarbons). Thus, the agreement between  $Z_{\text{eff}}$  for  $\text{CH}_4$  and  $\text{CD}_4$  is consistent with the direct annihilation mechanism. However, the measurements show that  $Z_{\text{eff}}$  values are quite similar for protonated and deuterated forms of larger alkanes. Based on the estimates given above, these large values of  $Z_{\text{eff}}$  cannot be explained by direct annihilation.

In the context of the theory of resonant annihilation (Sec. III B), the corresponding annihilation rate should be proportional to the density of vibrational excitations. The substitution of deuterons for protons in the molecules studied here lowers the frequencies of the high-frequency vibrational modes significantly. Consequently, it increases  $\rho(E)$ , and one could anticipate that the resonant mechanism would predict significantly larger values of  $Z_{\text{eff}}$  for deuterated alkanes, which was not observed.

One explanation for these observations is that the coupling between the electron-positron degrees of freedom and nuclear motion is weak, effectively either reducing or completely shutting off the process of resonance formation. This coupling might also be smaller for the deuterated alkanes compared with protonated ones. In this case the capture width  $\Gamma_c$  might become very small, and if  $\Gamma_c < \Gamma_a$ , the regime described by Eq. (13) does not take place. Another possibility is that only lower frequency vibrational modes take part in the resonance process, and thus, contribute to the density factor  $D^{-1}$  in Eq. (13), although these are more difficult for the relatively light positron to excite. Deuteration will not have a large effect on the frequency of these modes, which are dominated by the masses of the carbon atoms. Therefore, the effective mean vibrational spacing  $D$  could be roughly the same for protonated and deuterated alkanes. Thus far we have not succeeded in devising a way to test the possible effect of these low-frequency modes on the annihilation process.

## B. Annihilation rates for partially fluorinated hydrocarbons

As reported previously, [1,3,5], large alkane molecules have very large annihilation rates,  $Z_{\text{eff}}$ , compared with the number of electrons  $Z$ . In contrast, the analogous perfluorinated alkanes have annihilation rates that are orders of magnitude smaller [18]. Besides this,  $Z_{\text{eff}}$  increases very rapidly with the size of the molecule, approximately as  $Z_{\text{eff}} \propto Z^5$ , for alkanes with 3–9 carbon atoms, whereas for perfluorocarbons it follows a much slower  $Z_{\text{eff}} \propto Z^{1.7}$ . This large difference in annihilation rates between hydrocarbons and fluorocarbons can potentially provide insights into the physical processes responsible for the annihilation. In order to pursue this issue, we studied annihilation in molecules in which the hydrogen atoms in hydrocarbons have been selectively replaced with fluorine atoms to form partially fluorinated hydrocarbons.

The measured annihilation rates for a selection of partially fluorinated hydrocarbons are listed in Table III. It is interesting that, within a given series, the molecule with a single fluorine atom has the highest annihilation rate. Further fluorination decreases the annihilation rate gradually, with the perfluorinated molecule having the lowest annihilation rate. We note that molecules with one fluorine atom are highly dipolar. Although the effect of a permanent dipole moment on the annihilation rate is not understood, empirical evidence [1] indicates that this does not account for the large increases in annihilation rates that are observed for the monofluorinated molecules. In particular, partially fluorinated molecules containing more than one fluorine have dipole moments comparable in magnitude or larger than that of the monofluorinated compound, but significantly smaller annihilation rates.

For larger alkanes, the high values of  $Z_{\text{eff}}$  and their strong dependence on the size of the molecule are consistent with the resonant annihilation mechanism with a positron affinity  $\epsilon_A \approx 5\omega$ , where  $\omega$  is the typical frequency of molecular vibrations excited in the positron capture (see estimates in Sec. I and III B). Fluorination reduces the vibrational frequencies

and increases the vibrational spectrum density at a given energy. This, together with the loss of symmetry of the molecule, could be the reason for the increase in  $Z_{\text{eff}}$  with the first fluorine substitution. However, the rapid decrease of  $Z_{\text{eff}}$  observed when several H atoms are replaced with fluorines can be interpreted as “switching off” of the resonant mechanism due to the fact that the positron-molecule binding becomes weaker and then disappears with the addition of fluorine atoms. Note that for heavier halogen-substituted alkanes the annihilation rates are much larger [1]. Both Cl and Br are much more attractive for positrons than F. Thus in this case, the resonant annihilation model predicts that there will be a softening of the vibrational spectrum, but no loss of positron binding.

For the smallest of the alkanes, methane, the annihilation rate is relatively small,  $Z_{\text{eff}} \sim 10^2$ , although much larger than the number of valence electrons. Combined with the sparse vibrational spectrum of the molecule, this can be interpreted as evidence that (i) for room-temperature positrons annihilation proceeds via the direct mechanism, and (ii) the direct annihilation rate is enhanced by the presence of a virtual level, or a weakly bound state, cf. Sec. III A. In the context of the zero-range potential model in Sec. III C, the variation of  $Z_{\text{eff}}$  is then consistent with the change in the position of this level, when hydrogen atoms are substituted by fluorines. To test this hypothesis, we plot in Fig. 3 the dependence of  $Z_{\text{eff}}^{(\text{dir})}(T)$  at room temperature on the position of the virtual/bound state, as represented by the parameter  $\kappa$ . It has been calculated using Eqs. (6), (8), and (9). Solid dots show measured values of  $Z_{\text{eff}}$  as a function of  $\kappa$  calculated in the zero-range potential model, Table I, second line. These values of  $\kappa$  for the five  $\text{CH}_{4-x}\text{F}_x$  molecules are determined by the parameters  $\kappa_{\text{H}}$  and  $\kappa_{\text{F}}$  that describe the interaction of the positron with isolated H and F atoms. In the second line of Table I we use  $\kappa_{\text{H}}$  and  $\kappa_{\text{F}}$  as free parameters and find that  $\kappa_{\text{H}} = -0.72$  and  $\kappa_{\text{F}} = -1.275$  give the best fits to the experimental data shown in Fig. 3.

The main feature in Fig. 3 is the maximum in the dependence of  $Z_{\text{eff}}$  on  $\kappa$ . It corresponds to  $\kappa = 0$  point, where the virtual level ( $\kappa < 0$ ) turns into a bound state ( $\kappa > 0$ ), and where the scattering length becomes infinite. The annihilation rate remains finite at  $\kappa = 0$  because we consider finite-temperature positrons [cf. Eq. (7) with  $k > 0$ ]. Therefore, in the context of the model, the dependence of  $Z_{\text{eff}}$  on the degree of fluorination can be understood as a gradual change in the position of the level, from a bound state in  $\text{CH}_4$  (maximal binding energy  $\epsilon_A = \kappa^2/2 \approx 28$  meV) and  $\text{CH}_3\text{F}$ , to the virtual levels in di-, tri-, and tetrafluoromethane. The small binding energy of methane explains why the vibrational resonances do not contribute to the annihilation rate. We note that there is a discrepancy between measured  $Z_{\text{eff}}$  and the calculation for larger negative values of  $\kappa$ . This may be a result of the assumptions used that individual hydrogen and fluorine atoms contribute equally to  $Z_{\text{eff}}$ . Also, for larger  $|\kappa|$  the zero-range potential model becomes less accurate. The main result of this study of annihilation in methane and its fluorosubstitutes is evidence that the bound level disappears as the number of fluorines is increased. This effect could explain the difference between very large  $Z_{\text{eff}}$  in larger alkanes, due to resonant annihilation, and orders of magnitude smaller  $Z_{\text{eff}}$  for perfluoroalkanes, where the resonant mechanism would be switched off by the absence of binding.



## C. Dependence of annihilation rates on positron temperature

### 1. Noble gas atoms

Annihilation rates as a function of positron temperature for noble gas atoms were measured previously [9]. These data for the temperature dependence of  $Z_{\text{eff}}$  were found to be in good agreement [9] with calculation by Van Reeth *et al.* for He [7] and calculation by McEachran *et al.* for Ne, Ar, Kr, and Xe [27]. The data are plotted in Fig. 4 in log-log scale. We relate the observed temperature dependences for these atoms to that expected for direct annihilation (cf., Sec. III A). We find that we are able to fit the data using Eqs. (6), (8) and (9) using the known dipole polarizabilities  $\alpha = 2.377, 11.08, 16.74, \text{ and } 27.06$  a.u. for Ne through Xe, respectively. The values of the scattering length  $a$  and the constant  $C$  are taken from the scattering calculations of McEachran *et al.* [27] for the  $s$  wave:  $a = -0.61, -5.3, -10.4, \text{ and } -45.3$  a.u., and  $C = 0.001, 0.60, 0.35, \text{ and } 0.005$  for Ne, Ar, Kr, and Xe, respectively. The only free parameter in the fits is  $R_a$ , and we determine it by comparison with experimental data in the range of positron temperatures  $T = 0.025\text{--}0.1$  eV, where Eq. (8) is valid. The fits shown by solid curves in Fig. 4 correspond to  $R_a = 3.2, 3.2, 4.2, \text{ and } 4.2$  a.u. for Ne, Ar, Kr, and Xe, respectively. We see that the direct annihilation mechanism gives an accurate description of the measured temperature dependences at low positron energies. The stronger temperature dependence observed for heavier noble gas atoms is caused by the increasing magnitudes of the scattering length from Ne to Xe. As seen from Eq. (8) this causes more rapid variation of the phase shift, and hence the cross section  $\sigma$ , which, for heavier noble gas atoms, gives a dominant contribution to  $Z_{\text{eff}}$  in Eq. (6). Large negative scattering lengths (i.e., small negative  $\kappa$  parameters) correspond to the existence of low-lying virtual  $s$  levels for positrons on Ar, Kr, and Xe. This in turn enhances the absolute values of the annihilation rates at low positron energies (cf.  $Z_{\text{eff}} = 33.8, 90.1, \text{ and } 401$  for Ar, Kr, and Xe, respectively, at room temperatures [1,16]). The data can also be fit accurately, over almost entire energy range, by a power law,  $Z_{\text{eff}}(T) \propto T^{-\xi}$  (dash-dotted and dashed lines in Fig. 4), with  $\xi = -0.036, -0.039, -0.23, -0.32, \text{ and } -0.67$  for He, Ne, Ar, Kr, and Xe, respectively.

### 2. Partially fluorinated hydrocarbons

Annihilation rates were measured as a function of positron temperature in an attempt to test the hypothesis that a large  $s$ -wave scattering cross section (small  $\kappa$ ) due to weakly bound or virtual positron states can explain the trend of  $Z_{\text{eff}}$  in the partially fluorinated hydrocarbons. A smaller value of  $\kappa$  for  $\text{CH}_3\text{F}$  as compared with that for  $\text{CH}_4$  would result in a larger value of  $Z_{\text{eff}}$ , and one would expect that  $Z_{\text{eff}}$  for  $\text{CH}_3\text{F}$  would have a more rapid temperature dependence at low temperatures, since its value of  $\kappa$  is smaller. Measurements for these molecules are presented in Fig. 5. As can be seen from the figure, the dependence of the annihilation rate on positron temperature is similar for  $\text{CH}_3\text{F}$  and  $\text{CH}_4$  at low temperatures. The dotted line shown in the figure is a fit to the low-temperature part of the data with the coefficient of  $-0.53$ , which is between those of Kr and Xe (Fig. 4). This indicates that the absolute value of positron scattering length for these molecules is probably between those of Kr and Xe.

In Fig. 6, the data are plotted on an absolute scale and compared with the analytical direct annihilation fits from Eqs. (6), (8), and (9), based on  $a = 1/\kappa$  values from Table I. In this comparison, the data and theory are in reasonable agreement at low positron temperatures (i.e., energies). In spite of a large difference in  $\kappa$  values for CH<sub>4</sub> and CH<sub>3</sub>F, the slopes of their temperature dependences are rather similar. The key point appears to be that due to the terms containing the dipole polarizability in Eq. (8), the temperature dependence of  $Z_{\text{eff}}$  increases, and this effect is more pronounced for methane which has a larger value of  $\kappa$  (which would otherwise, for  $\alpha = 0$ , give a rather flat temperature dependence). Thus, the data and model are in reasonable agreement – the model predicts similar positron temperature dependences of  $Z_{\text{eff}}$  for both species, even though they have different values of  $\kappa$ . The fact that the temperature dependences are so similar (i.e., as shown in Fig. 5) might have led to the conclusion that very similar parameters were responsible for this. However, in the context of the model presented here, this does not appear to be the case.

The fit in Fig. 6 gives  $\kappa = 0.045$  for methane, and the scattering length  $a = 22$  a.u. is comparable in magnitude to those of Kr ( $a = -10$ ) and Xe ( $a = -45$  [27], or  $a = -100$  [15]). The positive sign of  $a$  implies that the positron has a weakly bound state with CH<sub>4</sub>. As for CH<sub>3</sub>F, the fit gives  $\kappa = 0.01$  or so ( $a \sim 100$ ), which has a large uncertainty, because for  $\kappa^2/2 \ll k_B T$  the temperature dependence becomes insensitive to the precise value of  $\kappa$ . We should also point out that CH<sub>3</sub>F is a polar molecule and the dipole force changes the description of low-energy scattering.

### 3. Hydrocarbons and deuterated hydrocarbons

The annihilation rate,  $Z_{\text{eff}}$ , has recently been predicted for ethylene, C<sub>2</sub>H<sub>4</sub>, by da Silva *et al.*, using a large-scale numerical calculation which included short-range correlation of the positron and the molecular electrons [22]. In order to test this prediction, we measured the dependence of  $Z_{\text{eff}}$  on positron temperature, which is shown in Fig. 7. The experimental data are scaled with the room-temperature value of  $Z_{\text{eff}} = 1\,200$ , measured in a previous experiment, which has the uncertainty of 20% [1]. The theoretical calculation [22] is shown in Fig. 7 as a solid line, and it underestimates the data. The calculated values are also shown by the dashed line, which is obtained by multiplying the theory by a scale factor of 1.3. The data and calculation are in reasonable agreement. As pointed out in Ref. [22], the calculated value of  $Z_{\text{eff}}$  for C<sub>2</sub>H<sub>4</sub> is sensitive to the inclusion of electron-positron correlations. Thus the agreement between theory and experiment provides evidence that such correlations are important in determining the annihilation rate.

The calculations of da Silva *et al.* demonstrate a strong dependence of both the elastic cross section and  $Z_{\text{eff}}$  on the positron energy. We note that, in the framework of the model for direct annihilation presented above, this behavior can be interpreted as evidence for the existence of a virtual level for the positron on C<sub>2</sub>H<sub>4</sub> with  $\kappa = -0.05$ , and can be fitted using the formulae of Sec. III A. This value of  $\kappa$  is in agreement with the scattering length  $a = -18.5$  a.u. determined from the zero-energy limit of the elastic scattering cross section  $\sigma = 4\pi a^2$  presented in Ref. [22]. Thus, it appears that the large value of  $Z_{\text{eff}}$  for C<sub>2</sub>H<sub>4</sub> at low temperatures is due to the large scattering cross section  $\sigma$ . In relation to this, it is interesting to note that the increase of the annihilation rates for the molecules C<sub>2</sub>H<sub>6</sub>, C<sub>2</sub>H<sub>4</sub>, and C<sub>2</sub>H<sub>2</sub> ( $Z_{\text{eff}} = 660, 1200$ , and  $3160$ , respectively [1,2]) correlates with the increase in

the total scattering cross sections for low-energy positrons on these molecules, which were measured down to 0.7 eV by Sueoka and Mori [42]. This is consistent with the predictions of Eq. (6) for direct annihilation, as the elastic cross section  $\sigma$  dominates in the total scattering cross section at low positron energies. The term with  $\sigma$  also dominates in Eq. (6), since the scattering lengths are expected to be large for these targets.

We have measured the dependence of annihilation rate on positron temperature for the deuterated methane  $\text{CD}_4$ , and butane  $\text{C}_4\text{H}_{10}$ , and these data are compared with those for methane in Fig. 8.  $Z_{\text{eff}}$  for  $\text{CD}_4$  is quite similar to that of  $\text{CH}_4$ , see Sec. VC 2. The dependence for butane is similar as well, but with much greater absolute values of  $Z_{\text{eff}}$ . The dotted line shown in the figure is a fit to the low-temperature part of the data with the slope  $-0.55$ . At low temperatures, the dependence can be derived from Eq. (13) to follow  $1/\sqrt{T}$  law for the resonant annihilation ( $s$  wave). The origin of the plateau in  $Z_{\text{eff}}$  that is observed at larger values of positron temperature is unclear. It could be due to higher partial-wave contributions to the resonant annihilation which emerge as  $T$ ,  $T^2$ , etc. for  $p$ ,  $d$ , etc. partial waves, respectively. However, if these contributions were present, the exponent in the power-law dependence of  $Z_{\text{eff}}$  on temperature would appear to be less than 0.5, and this is not observed. In smaller molecules where direct annihilation is expected to dominate at low positron temperatures, the plateau could result from both the direct contribution of the higher partial waves and from excitation of vibrational resonances by the positron. We note, however, that this interpretation does not provide an obvious explanation for the fact that the temperature dependence of  $Z_{\text{eff}}$  for  $\text{CH}_4$ ,  $\text{CD}_4$ , and  $\text{C}_4\text{H}_{10}$  are all so similar, and so several unanswered questions remain.

We had hoped that this study of the dependence of annihilation on positron energy would aid in distinguishing the two annihilation mechanisms considered here. At present, this is not the case. Whether there is a more universal picture that describes the self-similar temperature dependences that are observed remains to be seen. One interesting facet of the data is that no plateau has been seen in  $Z_{\text{eff}}$  for  $\text{CH}_3\text{F}$ , suggesting that further studies of the temperature dependence of  $Z_{\text{eff}}$  for a wider variety of molecules might be useful in determining the origin of the physical phenomena responsible for this feature of the data.

## D. Phenomenological models

As discussed in Sec. II, phenomenological models have been proposed in the past. We discuss two of these models, including one proposed by Laricchia and Wilkin [43,44], by testing their predictive values in comparison with our experimental data [1].

### 1. The scaling relation of Murphy and Surko

Murphy and Surko observed a scaling relation between the logarithm of  $Z_{\text{eff}}$  and the quantity  $(E_i - E_{\text{Ps}})$ , where  $E_i$  is the ionization energy of the atom or molecule and  $E_{\text{Ps}}$  is the binding energy of a positronium atom. This scaling is valid for all the atoms and single-bonded nonpolar molecules [18]. In particular,

$$\ln(Z_{\text{eff}}) = A(E_i - E_{\text{Ps}})^{-1}, \quad (18)$$

where  $A$  is a positive constant. This scaling is illustrated in Fig. 9 for comparison with other models. The peak-to-peak spread in measured  $Z_{\text{eff}}$  values is generally better than one order of magnitude. There is no apparent distinction between atoms and molecules or any change in the scaling at values of  $Z_{\text{eff}} \sim 10^3$ . To the extent that this simple relation matches the data, this scaling indicates that it is the electronic structure of the atom and the molecule that determines the annihilation rate, and other aspects of atomic and molecular structure, such as the character of the vibrational modes, play a relatively minor role in determining the annihilation rate.

Murphy and Surko [18] found that this scaling was not applicable to other molecules, such as polar molecules and those containing double and triple bonds. For these species, there are different ionization potentials for different bonds. While the authors found that using other than the lowest ionization potential improved the correlation of  $Z_{\text{eff}}$  with  $(E_i - E_{\text{Ps}})^{-1}$ , they considered such a model to have too much ambiguity to be useful.

## 2. The Laricchia-Wilkin model

Laricchia and Wilkin modeled the annihilation rate as follows [43]. They begin by arguing that energy conservation can be violated for a time interval,  $\Delta t$ , given by the uncertainty principle, and conclude that virtual positronium can be formed for a time

$$\Delta t = \frac{\hbar}{|E - E_i + E_{\text{Ps}}|}, \quad (19)$$

where  $E$  is the kinetic energy of the positron. They consider the total annihilation rate to be the sum of direct annihilation and the annihilation of virtual positronium due to “self” and “pickoff” annihilation. This is formulated as

$$Z_{\text{eff}} = \frac{\sigma v}{\pi r_0^2 c} \{ \gamma [1 - \exp(-\lambda\tau)] + (1 - \gamma) [1 - \exp(-\Delta t(\lambda_{sa} + \lambda_{po}))] \}, \quad (20)$$

where  $\gamma$  is the fraction of direct annihilation,  $\lambda$  is the direct annihilation rate,  $\tau$  is the positron-atom or positron-molecule interaction time,  $\lambda_{sa} = 2 \times 10^9 \text{ s}^{-1}$  is the self annihilation rate, and  $\lambda_{po}$  is the pickoff annihilation rate. It can be noted that the first term (direct annihilation contribution) in Eq. (20) is identical to Eq. (4) with the factor of  $\gamma$ . The direct annihilation rate can be calculated from the spin-averaged Dirac rate of  $\lambda = \pi r_0^2 c n_e$ , where the  $n_e$  is the electron density. They chose to estimate the electron density by putting all of valence electrons  $Z_v$  in a sphere of the size given by the Bohr radius,  $a_0$ . Thus

$$n_e = \frac{3Z_v}{4\pi a_0^3}, \quad (21)$$

and  $\lambda = 3r_0^2 c Z_v / (4a_0^3)$ . In their model, they consider pickoff annihilation to mean that the positron in the positronium atom annihilates with a atomic or molecular electron other than the electron forming the positronium atom. Laricchia and Wilkin assumed that this rate is enhanced by the atomic or molecular polarizability  $\alpha$

$$\lambda_{po} = \alpha \lambda = \frac{3r_0^2 c Z_v \alpha}{4a_0^3}. \quad (22)$$

The value of  $\gamma$  is estimated as  $\gamma = \exp(-\Delta t/\tau)$ , where the interaction time is taken as  $\tau = a_0/v$  for this approximation. The collision cross section is approximated by

$$\sigma = (10^{-15}\alpha) \text{ cm}^2, \quad (23)$$

with  $\alpha$  in unit of  $\text{\AA}^3$  in Ref. [43]. In Ref. [44], Laricchia and Wilkin chose to modify the assumed cross section by an additional factor,

$$\sigma = [10^{-16}\alpha(1 + \alpha)] \text{ cm}^2, \quad (24)$$

arguing the collision cross section will scale as  $\sigma \propto \sin^2(\delta_0)$ , where  $\delta_0$  is the phase shift [45]. We note that the factor  $(1 + \alpha)$  introduces another numerical constant for the relative weight of the two terms (which the authors choose to be 1).

Figure 10 shows the correlation of experimental  $Z_{\text{eff}}$  with the quantity calculated with Eq. (20) using the cross section Eq. (23) for the same atoms and molecules plotted in Fig. 9. The predicted values of  $Z_{\text{eff}}$  of noble gases correlate reasonably well. The model underestimates the observed values for alkane molecules by an order of magnitude, while it overestimates those for perfluorinated molecules by as much or more. Figure 11 shows the predicted values calculated using Eq. (24) for the same atoms and molecules. While this scaling improves the agreement for the alkanes, it results in poorer agreement for the perfluorinated compounds. Comparing Figs. 9, 10, and 11, we conclude that the scaling proposed by Murphy and Surko, although not perfect, is a better predictive parameter for atoms and single-bonded nonpolar molecules.

Murphy *et al.* observed that the scaling they proposed in Ref. [18] is not valid for polar molecules and molecules with double and/or triple bonds (see Ref. [1] for further analysis). Figures 12 and 13 show the predicted values calculated for the Laricchia-Wilkin model, using Eq. (20) and the cross section of Eqs. (23) and (24), respectively, for all available data. The values calculated from these two models correlate as well to all of the data as they do to the data for atoms and single-bonded molecules. The largest discrepancies are underestimates of the alkanes and overestimates of the values for the perfluorinated molecules. In this more general comparison, the predictions for the partially fluorinated hydrocarbons fall naturally in between these two groups of molecules.

### 3. Remarks and one more scaling relation

The model by Laricchia and Wilkin appears to us to include questionable assumptions. One such assumption is that all of the valence electrons are concentrated in a sphere of radius  $a_0$  [i.e., Eq. (21)], which is much smaller than the size of the molecule. This clearly overestimates the electron density. Yet the high annihilation rates predicted by this model are due in large part to this assumption. The enhancement of pickoff annihilation by the polarizability factor [Eq. (22)] might also be questioned, since  $\gamma$ -ray spectral measurements indicate that the positron wave function is distributed rather evenly over molecular species. [2]. Finally, the form of the cross section given by Eq. (24) introduces one additional parameter and does not appear to improve substantially the agreement with the available data.

The model by Laricchia and Wilkin predicts a divergence of annihilation rate at the positronium formation threshold, where the positron energy  $E = E_i - E_{\text{Ps}}$ . An *ab initio* calculation by Humberston and Van Reeth also predicts a divergence of annihilation rate at the positronium formation threshold [46,47]. The divergence found by Humberston and Van Reeth can also be derived from the diagrammatic expansion of the annihilation rate, Eq. (14) and Fig. 10 of Ref. [15]. However, the singular behavior of annihilation rate near the positronium formation threshold in the latter two calculations is of the form  $Z_{\text{eff}} \propto |E - E_i + E_{\text{Ps}}|^{-1/2}$ . It is qualitatively different than the singular behavior predicted by the Laricchia-Wilkin model, which is of the form  $Z_{\text{eff}} \propto |E - E_i + E_{\text{Ps}}|^{-1}$ . We note that it is now possible that positron annihilation in this energy range can be investigated experimentally in a precise manner using the intense, cold positron beam recently developed by Gilbert *et al.* [10]. These experiments are now in preparation.

Finally, we considered whether we might obtain agreement similar to that for the Laricchia-Wilkin model (i.e., Figs. 12 and 13), for all the available atomic and molecular data using a *purely empirical* model with fewer parameters. Plotted in Fig. 14 is  $Z_{\text{eff}}$  against  $\alpha/(E_i - E_{\text{Ps}})$ . We note that, while the correlation is not linear on a log-linear scale, it is as good as those shown in Figs. 12 and 13, and the model uses only one parameter (i.e., the polarizability) besides the quantity  $E_i - E_{\text{Ps}}$ . The fact that inclusion of  $\alpha$  in the scaling improves the correlation over  $(E_i - E_{\text{Ps}})^{-1}$  may reflect the importance of the collision cross section in the annihilation process.

## VI. CONCLUDING REMARKS

We have conducted new experimental studies of positron annihilation on molecules. We have also considered theoretically two mechanisms which could contribute to the large annihilation rates that are observed. Our estimates indicate that the direct annihilation mechanism is capable of giving  $Z_{\text{eff}} \sim 10^3$ . The resonant annihilation mechanism, which involves positron capture into the vibrationally excited states of the positron-molecule complex, appears at least in principle to be able to produce values of  $Z_{\text{eff}}$  as large as  $10^8$ . This mechanism is analogous to the electron-molecule capture mechanism thought to be responsible for very large dissociative attachment rates in some molecules.

In the case of direct annihilation, enhanced rates can be observed if there are weakly bound states or low-lying virtual levels. The annihilation rates for hydrocarbons with various degrees of fluorination were measured in order to test the predictions of this model. It was found that molecules with one fluorine have the largest annihilation rates, and successive fluorination monotonically decreases the rates. This trend was explored in detail for methane and its fluoro-derivatives and appears to be consistent with the simple zero-range potential calculations presented here. The model suggests that the first two members of the  $\text{CH}_{4-x}\text{F}_x$  series form weakly bound states with the positron, whereas for  $x = 2-4$  the molecules have only a virtual level for the positron. The dependence on temperature of the measured annihilation rates for methane and fluoromethane were found to be rather similar at low positron temperatures. Within the context of the direct annihilation mechanism, this is interpreted as a competition between the effect of a low value of  $\kappa$  for fluoromethane and a larger effect of the dipole polarizability for methane.

For larger molecules that possess a broad spectrum of vibrational resonances, we conjectured that the resonant annihilation mechanism is dominant. In this case, the absence of positron binding in the larger perfluorinated alkanes can explain the large difference in  $Z_{\text{eff}}$  values for these compounds as compared with alkanes which, according to the estimates discussed here, appear to be able to bind positrons. This resonant annihilation mechanism involves the formation of long-lived positron-molecule compounds through transfer of the positron's energy to the molecular vibrational modes. To test this model, measurements of annihilation rates of deuterated alkanes were made and compared to those of protonated ones. It was found that the deuterated alkanes have similar annihilation rates to the protonated ones. Thus this test did not confirm the predictions of the simplest interpretation of this model for the alkanes. We note that deuteration of benzene molecules did produce some changes in  $Z_{\text{eff}}$ . Thus the overall result of these tests is inconclusive.

Data were presented for the dependence of annihilation rates on positron temperature. Empirically, we noted similarities in the data for methane, deuterated methane, and butane, over a relatively wide range of positron temperatures, and for methane and fluoromethane at low positron temperatures. The dependence of annihilation rates on positron temperature follows power law with the coefficients of -0.53 for the combined data of methane and fluoromethane, and -0.55 for those of methane, deuterated methane, and butane. We find that we are able to explain these data within the context of simple models of direct and resonant annihilation described above. However this explanation required using (specific values of) a number of parameters, and did not provide universal explanations for these trends. Whether there is a more general theoretical framework to explain these dependences appears to us to be an open question which might benefit from further scrutiny.

The two possible annihilation mechanisms that are considered theoretically in this paper do not involve Ps formation in a direct way, since it is forbidden by energy considerations for low-energy positrons and atoms or molecules with  $E_i > E_{\text{Ps}}$ . In addition, one of the two mechanisms directly involves the molecular vibrations. In contrast, the empirical scaling described by Eq. (18) seems to indicate that the dominant mechanism for enhanced annihilation rates involves only the electronic structure of the atom or molecule (i.e., not the molecular vibrational modes). We are not aware of any theoretical framework that has these characteristics, and so we can offer only a couple of vague suggestions. If there were low-lying *electronic* excitations of a positron-atom or molecule complex, then a resonance model, such as that described above, might be possible, with the resonant modes now electronic, as opposed to vibrational, in nature. To our knowledge, there is no analogous phenomenon involving low-lying electronic excitations in electron-atom or electron-molecule interactions, and so the positron would have to play a fundamental role in these modes. We have speculated previously that the states might be thought of as a Ps atom moving in the field of the positively charged atomic or molecular ion [18].

The positron annihilation rate is proportional to the overlap of positron and electron wave functions. Thus, the short-range correlation between the positron and an electron is important. It poses a challenge to theory to include short-range correlation into the scattering problem. As discussed above, recent advances in computational approaches have enabled large-scale calculations of positron-molecule interactions to be carried out for small molecules such as ethylene. The agreement between theory and experiment for ethylene, as illustrated in Fig. 7, is encouraging [22]. This comparison provides support for the

importance of short-range electron-positron correlations in determining annihilation rates. Vibrational motion is not included in these calculations, and the estimates presented above indicate that these vibrational excitations are crucial in obtaining  $Z_{\text{eff}}$  values larger than about  $10^3$ . If the numerical calculations could be done for larger molecules, one could test this prediction.

Phenomenological models, including the model proposed by Laricchia and Wilkin [43,44], were analyzed using our experimental data. Their model predicts the observed annihilation rates reasonably well. However, the annihilation rates predicted by this model appear to us to arise from questionable assumptions. In Sec. V D 3, we proposed a new scaling with the parameter,  $\alpha/(E_i - E_{\text{Ps}})$ . This scaling exhibits a somewhat better correlation with measured values of  $Z_{\text{eff}}$  than the model by Laricchia and Wilkin. Nevertheless, we note that this new scaling is purely empirical, and its physical meaning is unclear. It was conjectured previously that the strong dependence of  $Z_{\text{eff}}$  on  $(E_i - E_{\text{Ps}})$  might indicate that the positron interacting with an atom or a molecule could be thought of as a highly correlated electron-positron pair moving in the field of the resulting positive ion [18]. The inclusion of the factor  $\alpha$  could mean that the collision cross section is also an important parameter in determining annihilation rate.

In conclusion, we do not find a ready and universal explanation for the anomalously large positron annihilation rates of organic molecules that have been observed in many experiments and for a wide range of molecules. Nevertheless, advances in the experimental measurements and formulating a theoretical framework for this problem have provided new insights. They place new constraints on theoretical models of this phenomenon.

## ACKNOWLEDGMENTS

We thank E. A. Jerzewski for expert technical assistance. The work at the University of California, San Diego is supported by the National Science Foundation, grant # PHY-9600407. One of us (G. G.) would like to thank S. Buckman, V. Flambaum, M. Kuchiev and O. Sushkov for useful discussions, and acknowledge support of the Australian Research Council.



## REFERENCES

- \* Current address: University of California, San Francisco, Physics Research Laboratory, 389 Oyster Point Blvd., Suite #1, South San Francisco, CA 94080
- † Current address: First Point Scientific Inc., 5330 Derry Avenue, Suite J, Agoura Hills, CA 91301
- ‡ Current address: Kasernenstrasse 8 A-7000 Eisenstadt, Austria
- § Corresponding author: csurko@ucsd.edu.
- [1] K. Iwata *et al.*, Physical Review A **51**, 473 (1995).
- [2] K. Iwata, R. G. Greaves, and C. M. Surko, Phys. Rev. A **55**, 3586 (1997).
- [3] D. A. L. Paul and L. Saint-Pierre, Physical Review Letters **11**, 493 (1963).
- [4] G. R. Heyland, M. Charlton, T. C. Griffith, and G. L. Wright, Can. J. Phys. **60**, 503 (1982).
- [5] C. M. Surko, A. Passner, M. Leventhal, and F. J. Wysocki, Phys. Rev. Lett. **61**, 1831 (1988).
- [6] C. M. Surko, M. Leventhal, and A. Passner, Phys. Rev. Lett. **62**, 901 (1989).
- [7] P. Van Reeth *et al.*, J. Phys. B **29**, L465 (1996).
- [8] M. D. Tinkle *et al.*, Phys. Rev. Lett. **72**, 352 (1994).
- [9] C. Kurz, R. G. Greaves, and C. M. Surko, Phys. Rev. Lett. **77**, 2929 (1996).
- [10] S. J. Gilbert, C. Kurz, R. G. Greaves, and C. M. Surko, Appl. Phys. Lett. **70**, 1944 (1997); C. Kurz, S. J. Gilbert, R. G. Greaves, and C. M. Surko, Nucl. Instrum. Methods B, **143**, 188 (1998); S. J. Gilbert, R. G. Greaves, and C. M. Surko, Phys. Rev. Lett., submitted.
- [11] J. W. Humberston and J. B. G. Wallace, J. Phys. B **5**, 1138 (1972).
- [12] Here we use “low-lying” and “shallow” to mean energies much less than typical atomic ones ( $\sim$  Ryd). More accurately,  $\kappa^{-1}$  must be larger than the size of the target, where  $\kappa$  is the parameter of the virtual or bound level:  $\varepsilon_0 = \pm\kappa^2/2$  (in a.u.).
- [13] V. I. Goldanskii and Yu. S. Sayasov, Phys. Lett. **13** 300 (1964).
- [14] V. A. Dzuba, V. V. Flambaum, W. A. King, B. N. Miller, and O. P. Sushkov, Phys. Scripta T **46**, 248 (1993).
- [15] V. A. Dzuba, V. V. Flambaum, G. F. Gribakin, and W. A. King, J. Phys. B **29**, 3151 (1996).
- [16] T. J. Murphy and C. M. Surko, J. Phys. B **23**, L727 (1990).
- [17] See D. T. Alle, M. J. Brennan, and S. J. Buckman, J. Phys. B **29**, L277 (1996), and references therein.
- [18] T. J. Murphy and C. M. Surko, Phys. Rev. Lett. **67**, 2954 (1991).
- [19] M. Leventhal, A. Passner, and C. Surko, in *Annihilation in Gases and Galaxies*, R.J. Drachman, ed., NASA Conf. Pub. Number **3058**, 1990, pp. 273-284.
- [20] V. A. Dzuba, V. V. Flambaum, G. F. Gribakin, and W. A. King, Phys. Rev. A **52**, 4541 (1995).
- [21] G. G. Ryzhikh and J. Mitroy, Phys. Rev. Lett. **79**, 4124 (1997); J. Phys. B **31** L401 (1998); **31** 4459 (1998); G. G. Ryzhikh, J. Mitroy, and K. Varga 1998 J. Phys. B **31** L265 (1998); J. Mitroy, private communication.
- [22] E. P. da Silva, J. S. E. Germane, and M. A. P. Lima, Physical Review Letters **77**, 1028 (1996).

- [23] K. Iwata, G. F. Gribakin, R. G. Greaves, and C. M. Surko, *Phys. Rev. Lett.* **79**, 39 (1997).
- [24] G. F. Gribakin, manuscript in preparation.
- [25] A. I. Akhiezer and V. B. Berestetskii, *Quantum Electrodynamics* (Interscience Publishers, New York, 1965).
- [26] P. M. Smith and D. A. L. Paul, *Can. J. Phys.* **48**, 2984 (1970).
- [27] R. P. McEachran, A. G. Ryman, and A. D. Stauffer, *J. Phys. B* **11**, 551 (1978); **12**, 1031 (1979); R. P. McEachran, A. D. Stauffer, and L. E. M. Campbell; *ibid* **13**, 1281 (1980).
- [28] L. D. Landau and E. M. Lifshitz, *Quantum mechanics*, 3rd ed. (Pergamon Press, Oxford, UK, 1977), p. 548.
- [29] T. F. O'Malley, L. Spruch, and L. Rosenberg, *J. Math. Phys.* **2**, 491 (1961). In Eq. (8) the positive constant  $C$  determines the contribution of the  $k^2$  term in the expansion of  $k \cot \delta_0$ . As shown by O'Malley *et al.*, this quantity can be expressed in terms of  $a$ ,  $\alpha$  and the modified effective range,  $r_{p0}$ .
- [30] G. K. Ivanov, *Dokl. Phys. Chem.* **291** 1048 (1986).
- [31] L. G. Christophorou, K. S. Gant, and V. E. Anderson, *Journal of Chemical Society; Faraday Transaction II* **73**, 804 (1977).
- [32] L. G. Christophorou, A. Hadjiantoniou, and J. G. Carter, *Journal of Chemical Society; Faraday Transaction II* **69**, 1713 (1973).
- [33] Y. N. Demkov and V. N. Ostrovskii, *Zero-range potentials and their applications in atomic physics* (Plenum Press, New York, 1988).
- [34] B. M. Smirnov and O. B. Firsov, *Sov. Phys. JETP* **20**, 156 (1965).
- [35] C. Schwartz, *Physical Review* **124**, 1468 (1961).
- [36] D. M. Schrader, *Physical Review A* **20**, 933 (1979).
- [37] H. J. M. Bowen, *Tables of interatomic distances and configuration in molecules and ions* (Chemical Society, London, 1958).
- [38] A. P. Mills, Jr. and E. M. Gullikson, *Applied Physics Letters* **49**, 1121 (1986).
- [39] R. G. Greaves and C. M. Surko, *Canadian Journal of Physics* **51**, 445 (1996).
- [40] T. J. Murphy and C. M. Surko, *Physical Review A* **46**, 5696 (1992).
- [41] R. G. Greaves, M. D. Tinkle, and C. M. Surko, *Physics of Plasmas* **1**, 1439 (1994).
- [42] O. Sueoka and S. Mori, *J. Phys. B* **22**, 963 (1989).
- [43] G. Laricchia and C. Wilkin, *Phys. Rev. Lett.* **79**, 2241 (1997).
- [44] G. Laricchia and C. Wilkin, *Nucl. Instrum. Methods B* **143**, 135 (1998).
- [45] G. Laricchia, private communication.
- [46] P. Van Reeth and J. W. Humberston, *J. Phys. B* **31**, L231-238 (1998).
- [47] J. W. Humberston and P. Van Reeth, *Nucl. Instrum. Methods B* **143**, 127 (1998).

## FIGURES

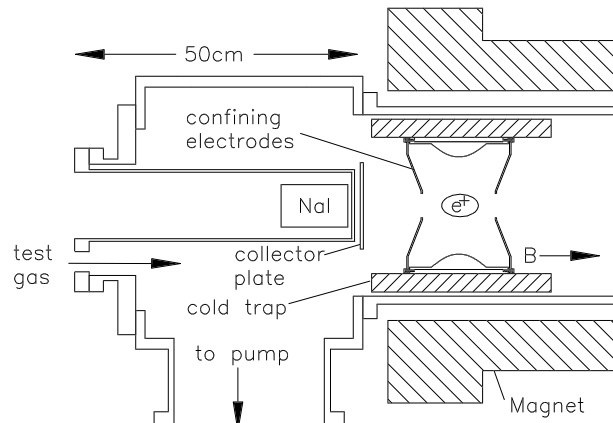


FIG. 1. Final stage of the positron trap showing schematically an accumulated positron cloud and the  $\gamma$ -ray detector.

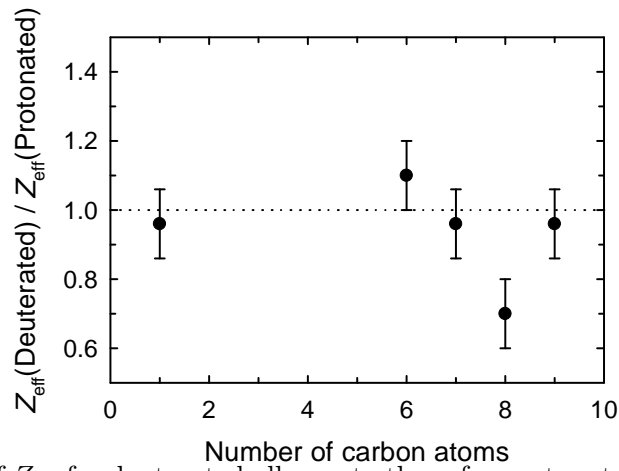


FIG. 2. The ratios of  $Z_{\text{eff}}$  for deuterated alkanes to those for protonated alkanes plotted against the number of carbon atoms,  $j$ .

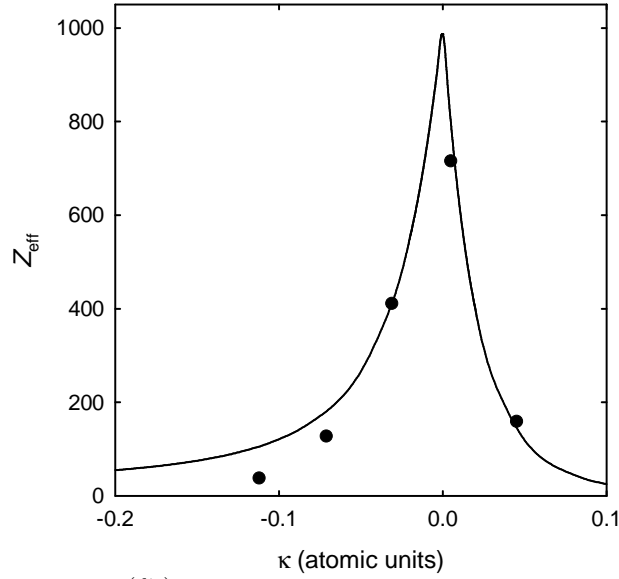


FIG. 3. The dependence of  $Z_{\text{eff}}^{(\text{dir})}(T)$  at room temperature on the parameter  $\kappa$  of the virtual and bound  $s$  state, calculated from Eqs. (6), (8) and (9) using  $F = 0.93$ ,  $R_a = 4$ ,  $\alpha = 17.6$  (polarizability of  $\text{CH}_4$ ), and  $C = 1$ . The solid circles are values of  $Z_{\text{eff}}$  for  $\text{CF}_4$ ,  $\text{CHF}_3$ ,  $\text{CH}_2\text{F}_2$ ,  $\text{CH}_3\text{F}$ , and  $\text{CH}_4$  (from left to right) of the present experiment, normalized to  $Z_{\text{eff}} = 158.5$  (for  $\text{CH}_4$ ), plotted as a function of  $\kappa$  values obtained from the zero-range positron-molecule binding model, Table I, second line.

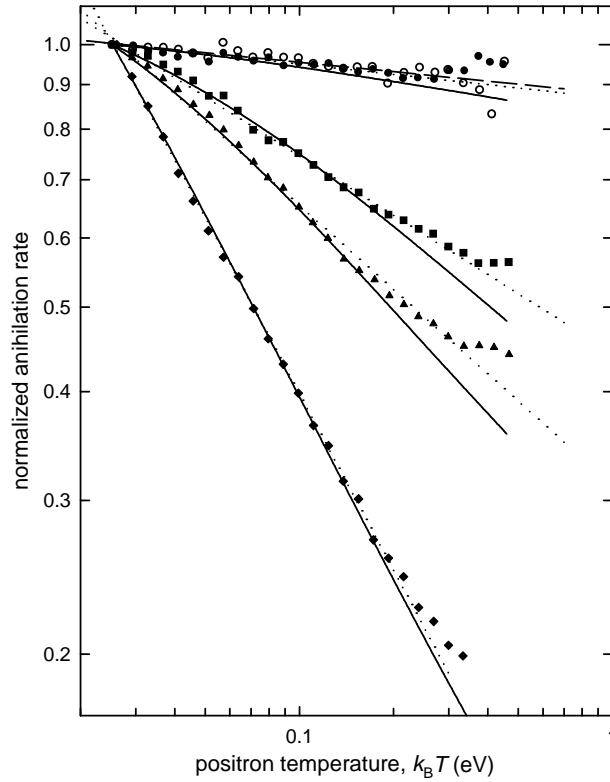


FIG. 4. Dependence of annihilation rates on positron temperature for noble gas atoms (data are from Ref. [9]): ( $\circ$ ) He, ( $\bullet$ ) Ne, (solid square) Ar, (solid triangle) Kr, and (solid diamond) Xe. The annihilation rates are normalized to their room-temperature values. The experimental data are fit with the direct annihilation formulas, Eqs. (6), (8), and (9) (solid curves). Power law fits to the low temperature parts of the data are also shown, corresponding to exponents of  $-0.036$  (He) (dash-dotted line),  $-0.039$  (Ne),  $-0.23$  (Ar),  $-0.32$  (Kr), and  $-0.67$  (Xe) (dashed lines).

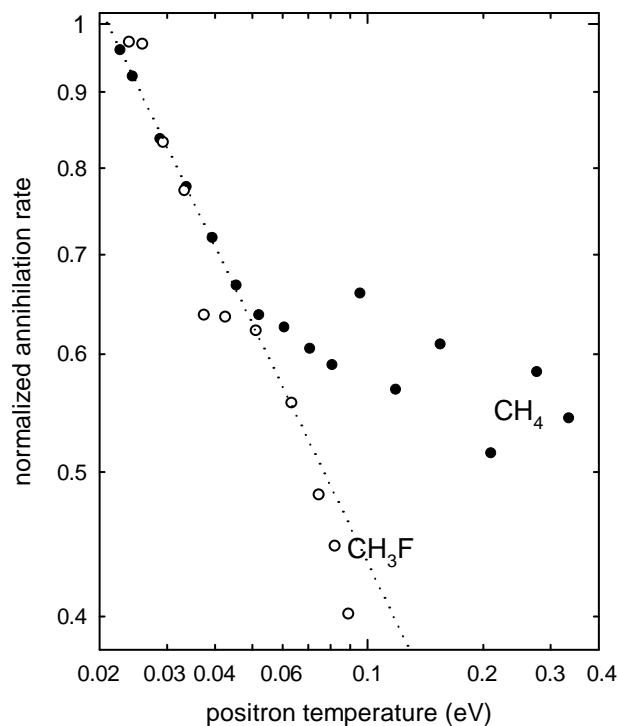


FIG. 5. Dependence of annihilation rates on positron temperature: ( $\bullet$ ) methane ( $\text{CH}_4$ ), and ( $\circ$ ) fluoromethane ( $\text{CH}_3\text{F}$ ). The annihilation rates are normalized to their room-temperature values. The dotted line ( $\cdots$ ) is a fit to the lower temperature data with the coefficient of  $-0.53$ .

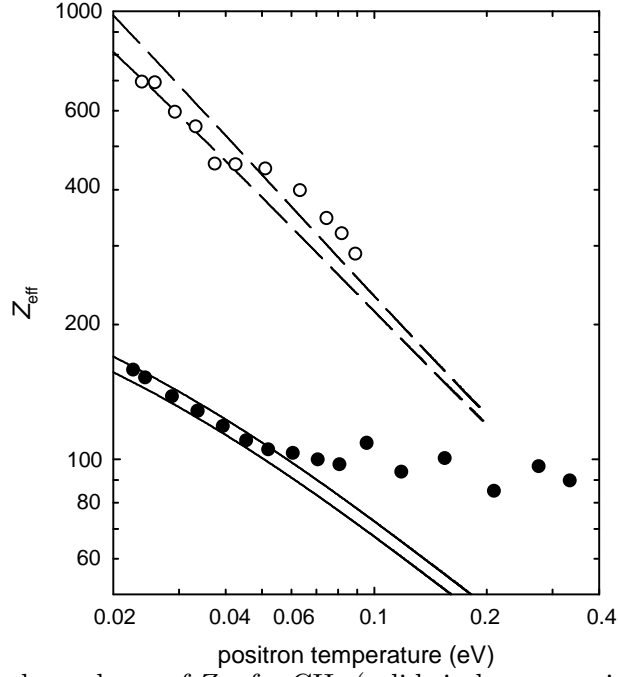


FIG. 6. Temperature dependence of  $Z_{\text{eff}}$  for  $\text{CH}_4$  (solid circles – experiment, solid lines – theory) and  $\text{CH}_3\text{F}$  (open circles – experiment, dashed lines – theory). The theoretical curves are obtained using  $R_a = 4$ ,  $\alpha = 17.6$ , and  $C = 1$ , and the following parameters. For  $\text{CH}_4$ :  $F = 1$ ,  $\kappa = 0.045$  (upper curve),  $F = 0.93$ ,  $\kappa = 0.0452$  (lower curve); for  $\text{CH}_3\text{F}$ :  $F = 0.93$ ,  $\kappa = 0.005$  (upper curve),  $F = 1$ ,  $\kappa = 0.01$  (lower curve).

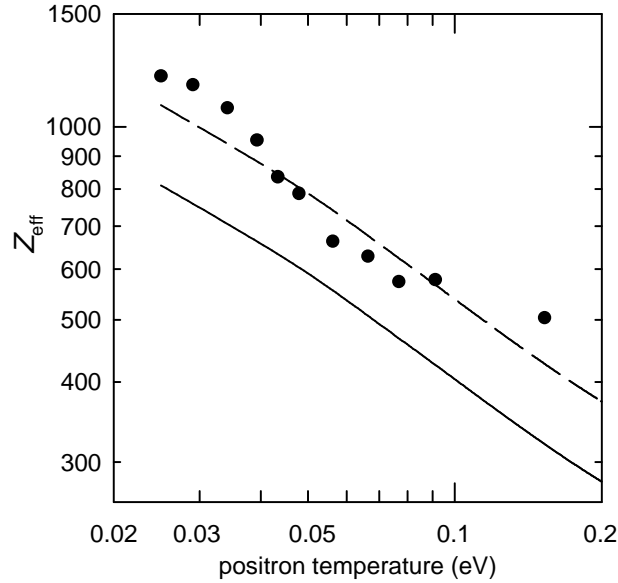


FIG. 7. Temperature dependence of the annihilation rate for ethylene; experiment ( $\bullet$ ) and calculation ( $-$ ) [22]. The dashed line ( $- - -$ ) is the calculation fit to the experimental data, which requires a scale factor of 1.3.

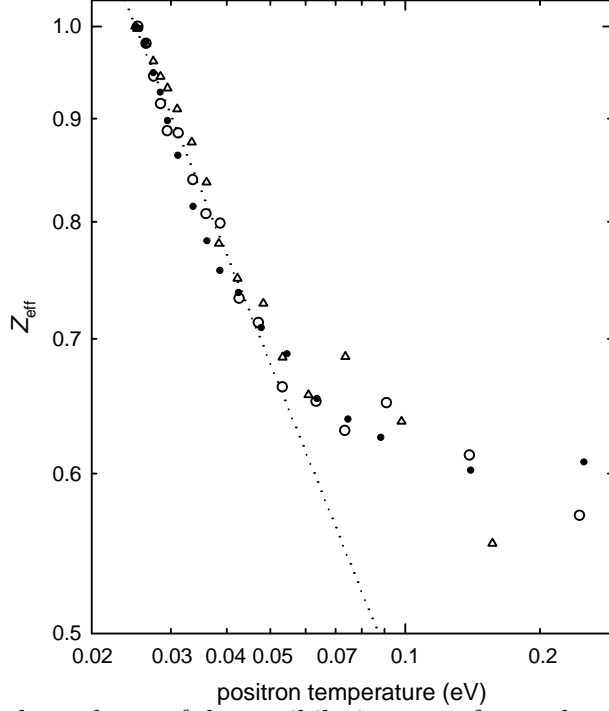


FIG. 8. Temperature dependence of the annihilation rates for methane ( $\circ$ ), deuterated methane ( $\triangle$ ), and butane ( $\bullet$ ). The dotted line ( $\cdots$ ) is a fit to the lower temperature data with the coefficient of  $-0.55$ . The theoretical fit for methane is shown in the previous figure. The data for butane show  $1/\sqrt{T}$  behavior at small temperatures, which is characteristic of the resonant annihilation.

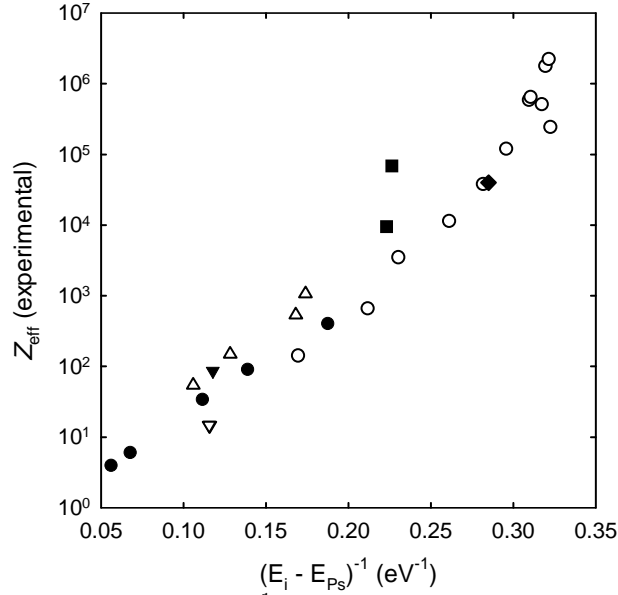


FIG. 9. Scaling of  $Z_{\text{eff}}$  with  $(E_i - E_{\text{Ps}})^{-1}$ . The data plotted are all the atoms and molecules for which physical parameters are available for calculation of the predictions of the other models discussed in Sec. VD: ( $\bullet$ ) noble gases, ( $\nabla$ )  $\text{H}_2$ , (solid triangle down)  $\text{SF}_6$ , ( $\circ$ ) alkanes, ( $\triangle$ ) perfluorinated alkanes, (solid square) perchlorinated alkanes, and (solid diamond)  $\text{CBr}_4$ .

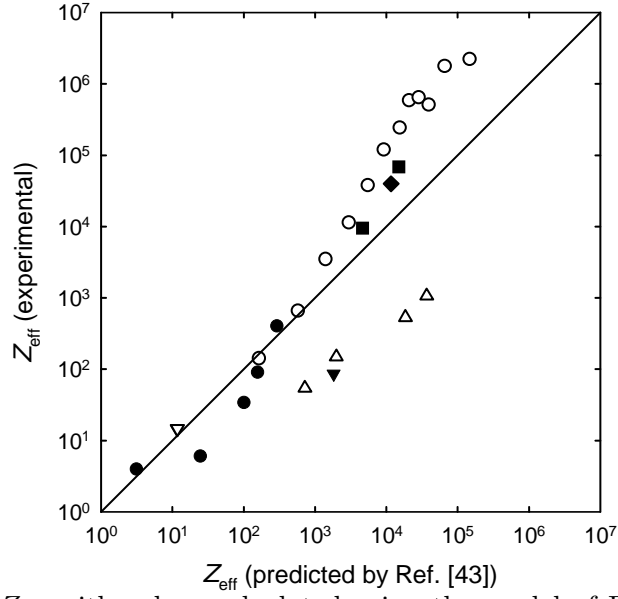


FIG. 10. Scaling of  $Z_{\text{eff}}$  with values calculated using the model of Ref. [43]. (—) is the line  $y = x$ . The same symbols are used as in Fig. 9.

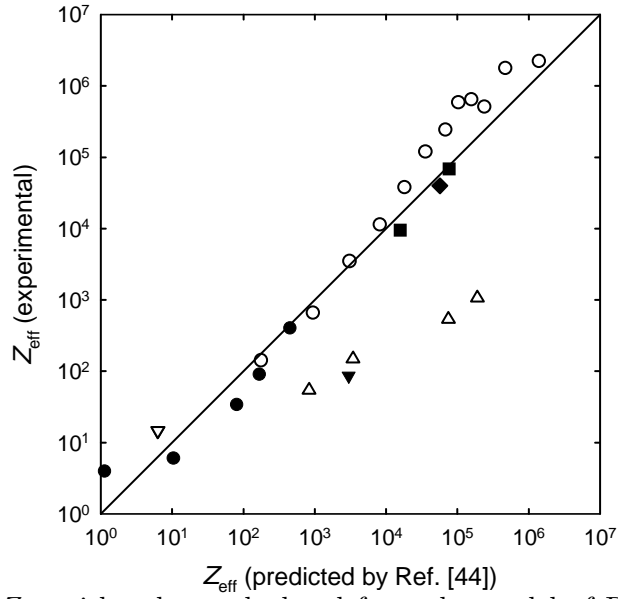


FIG. 11. Scaling of  $Z_{\text{eff}}$  with values calculated from the model of Ref. [44]. (—) is the line  $y = x$ . The same symbols are used as in Fig. 9.



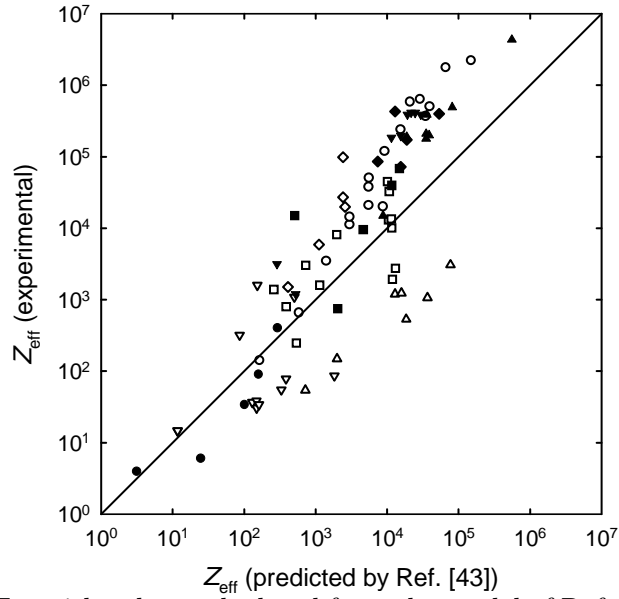


FIG. 12. Scaling of  $Z_{\text{eff}}$  with values calculated from the model of Ref. [43]: ( $\bullet$ ) noble gases, ( $\nabla$ ) inorganic molecules, ( $\circ$ ) alkanes, (solid triangle down) alkenes and acetylene, (solid triangle up) aromatic hydrocarbons, ( $\triangle$ ) perfluorinated alkanes, (solid square) perchlorinated alkanes,  $\text{CBr}_4$ ,  $\text{CH}_3\text{Cl}$ , and  $\text{CCl}_2\text{F}_2$ , ( $\diamond$ ) alcohols, carboxylic acids, ketones, (solid diamond) substituted benzenes, and ( $\square$ ) partially fluorinated hydrocarbons. (—) is the line  $y = x$ .

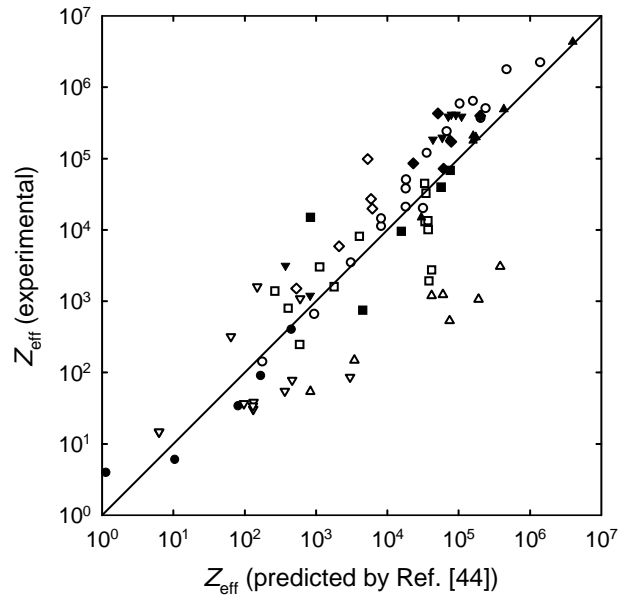


FIG. 13. Scaling of  $Z_{\text{eff}}$  with values calculated from the model of Ref. [44]. The same symbols are used as in Fig. 12.

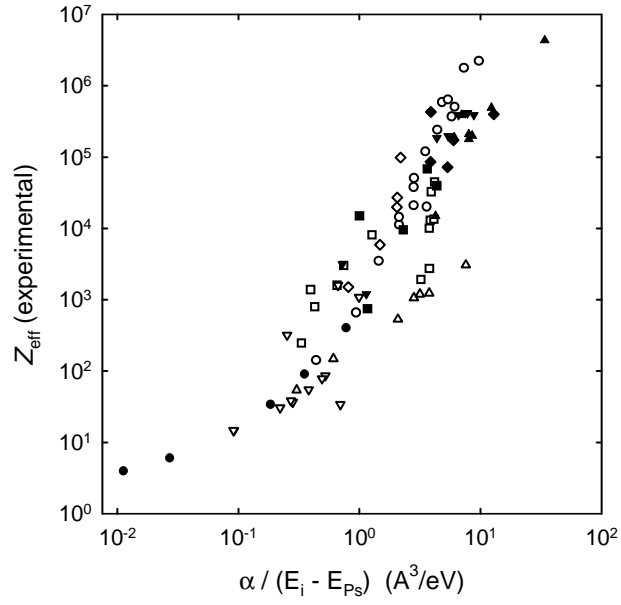


FIG. 14. Scaling of  $Z_{\text{eff}}$  with  $\alpha/(E_i - E_{Ps})$ . The same symbols are used as in Fig. 12.

## TABLES

TABLE I. Effect of fluorination on the parameter  $\kappa$  of the bound or virtual levels for positrons with the  $\text{CH}_{4-x}\text{F}_x$  molecules.

No. of F atoms	0	1	2	3	4
$\kappa^{\text{a}}$	0.111	0.053	-0.014	-0.103	-0.217
$\kappa^{\text{b}}$	0.0452	0.005	-0.031	-0.071	-0.112

<sup>a</sup> $\kappa_{\text{H}} = -0.5, \kappa_{\text{F}} = -2.0.$

<sup>b</sup> $\kappa_{\text{H}} = -0.72, \kappa_{\text{F}} = -1.275.$

TABLE II. Measured values of  $Z_{\text{eff}}$  for protonated and deuterated alkanes with number of carbon atoms,  $j$ . All values are measured in the positron trap. The last column is the ratio of  $Z_{\text{eff}}$  for deuterated alkanes to those for protonated alkanes.

Molecule	$j$	$\text{C}_j\text{H}_{2j+2}$	$Z_{\text{eff}}$	$\text{C}_j\text{D}_{2j+2}$	Ratio
Methane	1	222		214	0.96
Hexane	6	105 000		116 000	1.10
Heptane	7	355 000		341 000	0.96
Octane	8	585 000		408 000	0.70
Nonane	9	666 000		641 000	0.96

TABLE III. Values of  $Z_{\text{eff}}$  for partially fluorinated hydrocarbons.

Molecule	Formula	$Z$	$Z_{\text{eff}}$
Methane	$\text{CH}_4$	10	308
Methyl fluoride	$\text{CH}_3\text{F}$	18	1 390
Difluoromethane	$\text{CH}_2\text{F}_2$	26	799
Trifluoromethane	$\text{CHF}_3$	34	247
Carbon tetrafluoride	$\text{CF}_4$	42	73.5
Ethane	$\text{C}_2\text{H}_6$	18	1 780
Fluoroethane	$\text{C}_2\text{H}_5\text{F}$	26	3 030
1,1,1-Trifluoroethane	$\text{CF}_3\text{CH}_3$	42	1 600
1,1,2-Trifluoroethane	$\text{CHF}_2\text{CH}_2\text{F}$	42	1 510
1,1,1,2-Tetrafluoroethane	$\text{CF}_3\text{CH}_2\text{F}$	50	1 110
1,1,2,2-Tetrafluoroethane	$\text{CHF}_2\text{CHF}_2$	50	467
Hexafluoroethane	$\text{C}_2\text{F}_6$	66	149
Propane	$\text{C}_3\text{H}_8$	26	2 350
2,2-Difluoropropane	$\text{CH}_3\text{CF}_2\text{CH}_3$	42	8 130
1,1,1-Trifluoropropane	$\text{CF}_3\text{C}_2\text{H}_5$	50	3 350
Perfluoropropane	$\text{C}_3\text{F}_8$	90	317
Hexane	$\text{C}_6\text{H}_{14}$	50	151 000
1-Fluorohexane	$\text{CH}_2\text{FC}_5\text{H}_{11}$	58	269 000
Perfluorohexane	$\text{C}_6\text{F}_{14}$	162	630
Benzene	$\text{C}_6\text{H}_6$	42	20 300
Fluorobenzene	$\text{C}_6\text{H}_5\text{F}$	50	45 100
1,2-Difluorobenzene	$\text{C}_6\text{H}_4\text{F}_2$	58	32 800
1,3-Difluorobenzene	$\text{C}_6\text{H}_4\text{F}_2$	58	13 100
1,4-Difluorobenzene	$\text{C}_6\text{H}_4\text{F}_2$	58	13 500
1,2,4-Trifluorobenzene	$\text{C}_6\text{H}_3\text{F}_3$	66	10 100
1,2,4,5-Tetrafluorobenzene	$\text{C}_6\text{H}_2\text{F}_4$	74	2 760
Pentafluorobenzene	$\text{C}_6\text{HF}_5$	82	1 930
Hexafluorobenzene	$\text{C}_6\text{F}_6$	90	499